Egypt. J. Chem. **Vol. 65**, No. 11 pp. 641 – 664 (2022)

Egyptian Journal of Chemistry

http://ejchem.journals.ekb.eg/

Magnetic Nano-Organo-Philic Clay and Zeolite to Remove Municipal Carbonaceous Wastes in Matrouh Station

Yasser A.M. Abdulhady*

Hydro geochemistry dept., Water Treatment and Desalination Unit, Desert Research Center, Cairo, Egypt

Abstract

The iron nanocomposite of montmorillonite and zeolite in nano-sized as adsorbent with size 12-62 nm was carried by co-precipitation technology. Some carbonaceous compounds such as TSS/COD/BOD and TOC and also total nitrogen (TN), total phosphorous (TP) and total suspended solids (TSS) was studied. Pre-treatment analysis of raw clay and zeolite was done by acidification process. The prepared nanocomposite was characterized by X-ray diffraction (XRD) analysis; scanning electron microscopy (SEM), particle size distribution, and fourier transform infrared (FT-IR) spectroscopy and vibration sample magnetometry. This study focused on removal of COD, BOD, TOC and total nitrogen & phosphates by adsorption and desorption processes. The results showed that the maximum percentage removal of COD, BOD, TOC and TSS by using nanocomposite montmorillonite and zeolite/IONPs were 83.13 %, 88.07 %, 86.12 % and 79.2 % respectively. And also, for TN, TP and TSS were 73.74 %, 70.60 % and 79.21 %. The ratio values between COD/BOD5 & COD/TOC and TOC/BOD5 were 1.58, 1.63 and 0.97. Optimal conditions; Nanocomposite dosage: 5 g/l; Contact time: 30 min.; Temp.: 50oC; pH: 6.0. Adsorption data were reproduced by the Langmuir isotherm, where the carbonaceous compounds adsorption saturation capacity was determined as 72.04 and 206.61 mg/g respectively. The average adsorption free energy change was 2.880 kJ/mol, which indicated the occurrence of ionic exchange. The thermodynamic parameters implied that carbonaceous compounds adsorption was endothermic.

Key words: montmorillonite; zeolite; iron nanocomposite; wastewater treatment; municipal carbonaceous wastes.

1. INTRODUCTION

An effective purification method of clay minerals is by acidified treatment [1]. Suggested analytical method is depending on suspended clay in a phosphate solution. This method could be used for clay mineral through increase the proportion of montmorillonite in the clay from 30 % to 70 % by eliminating carbonates, quartz and other skeleton minerals [2]. Surface modifications of clay minerals have gained attention due to they let omit and replace by the production. There are varied methods to change 2:1 clay mineral: adsorption, ion exchange with inorganic & organic cations, connecting of inorganic and organic anions, mainly at the edges, coating of organic compounds, reaction with acids, poly (hydroxo metal) cations calcination and re-aggregation of some clay minerals, and physical treatments such as ultrasound, and plasma [3]. Among the different places of surface and groundwater contamination, the leachate from municipal solid waste one of the most important, because it produces a high concentrated liquid contains high concentrations of organic matter and inorganic matter like TDS, SS, phenols, chlorides, ammonia, and heavy metals. Surface and groundwater are polluted due to infiltration of leachate when it is not treated [4,5]. There are several ways that can be adopted for the treatment of Municipal Solid Waste (MSW) materials. The proposed treatment for the decrease the pollutants are physico-chemical method [6], coagulation [7], adsorption [8], ion exchange, chemical precipitation, bioremediation [9-11], constructed wetland [12-14]. There is a limitation for each treatment method about the cost, time; an alternative method was proposed for treatment. It is better to use carbonaceous material

*Corresponding author e-mail: yasser_vip6@hotmail.com.; (Yasser A.M. Abdulhady).
Receive Date: 09 January 2022; Revise Date: 06 March 2022; Accept Date: 10 March 2022.
DOI: 10.21608/EJCHEM.2022.115470.5240 .

in wastewater. Once such method is electrocoagulation process [15-17]. Electro-coagulation method may be used to treat liquid and solid waste by direct and indirect oxidation, reduction. It also offers environmental ecofriendly and since electrocoagulation process is made by electron exchange with the electrode surface, without the need for the addition of other chemical agents. Organic Fraction Municipal Solid Waste (OFMSW) is used as a feedstock for anaerobic digestion and source for biogas generation [18-19].The anaerobic treatment digestion of wastes may produce soil fertilizer [20]. OFMSW includes food waste, kitchen waste, leaf, grass clippings, flower trimmings and yard waste. Chemicals such as acids, base, and oxidants have been high efficiency to destroy natural contents [21]. Chemical treatment is used to breakdown the binding bonds in plant cell wall by employing strong acids, alkali or oxidants [22]. Alkali treatment makes solvation and saponification process [23].We need to large surface region to give substrates availability to anaerobes [24-25]. Ozonation is a method may be achieved along with enhanced hydrolysis rate. However, chemical treatment has less appropriate for easily biodegradable [26-27]. This study focused on removal of organic matter in terms of total organic content (TOC), chemical oxygen demand (COD) and biochemical oxygen demand (BOD). In addition to remove inorganic content such as and nitrates & Phosphates from the municipal solid waste by using adsorption technique. Insufficiently treated wastewater contains vast amounts of pollutants such as solids, organic and inorganic insoluble, and insoluble formulated particles, heavy metals, pathogenic microorganisms, and others. These pollutants may be toxic or mutagenic [28]. The disposal of partially treated and/or untreated wastewater into surface water cause potential or severe pollution and has adverse effects on the water, the health, and the environment [29]. Drainage wastewater treatment and reuse is an attractive option for blocking the gap in water needs, this is due to the diminishing of fresh water resources, rapid industrialization and recognition of new more harmful contaminants. In the last century, wastewater treatment entails the removal of solids (suspended, colloidal and floated), biodegradable organic matters, nutrients and elimination of pathogenic microorganisms [30]. The novality of research considered on synthetized new (Montmorillonite and Zeolite/IONPs) to achieve economic target for getting high reduction % performance of contaminants with low cost of adsorbent materials. This study was focused on removal of COD/BOD and TOC and also total nitrogen & phosphates by adsorption and desorption processes. The results showed that the maximum percentage removal of COD, BOD, TOC and total suspended solids (TSS) and ratio between COD/BOD_5 & COD/TOC and TOC/BOD_5.

2. EXPERIMENTAL AND MATERIALS

2.1. Materials

Ferric chloride hexahydrate ($FeCl_3.6H_2O$), ferrous chloride tetra-hydrate ($FeCl_2.4H_2O$), ammonium hydroxide (NH_4OH), NaOH, HCl, nitric acid, ethyl alcohol, and acetone purchased from Merck. Montmorillonite and raw zeolite were obtained from local supplier. Samples were collected from marsa matrouh city with municipal solid waste sterilized bottles covered with ice cubes and kept at 4 °C for analyzing the various parameters.

2.2. Procedure of Clay Purification

The first method is purification of local Egyptian clay mineral by acidification method. In our study, add to 100 g. of raw clay 1% HCl concentrations to remove excess percent of carbonate mainly and other several oxides and hydroxyls compounds. Modified suspensions were stirred for 2 h at a room temperature and afterwards decanted. The second step prepare to iron oxide from merging of ferrous and ferric inorganic salts prior to the reaction with NH_4OH and its amount was adjusted to obtain the bentonite/iron oxide weight ratios 3:1 and 6:1 with vigorous stirring with purified clay. Alkai concentrated added to solution to get new nanocomposite. Solution were washed with deionized water several times and then dried at 105°C temperature. Dried clay samples were crushed into powder. [31, 32].

2.3. Preparation of iron nanocomposite with montmorillonite/zeolite

In the present study, magnetic nanoparticles were prepared by the co-precipitation method. The magnetic nanoparticles were prepared from Iron (II) and Iron (III) (molar ratio of 1: 2) alkaline solution at the 80^oC temperature. A two-mouth 250 ml flask equipped with a magnetic stirrer was used for stirring

$FeCl_3.6H_2O$ (15 g) and $FeCl_2.4H_2O$ (6 g) in distilled water. Then, 250 ml of 2.5 M NaOH was added to the compound which was being rapidly stirred. The stirring continued for an hour at the 80^oC temperature. Finally, 200 ml of distilled water was used to wash the compound four times and ultimately, it was dissolved in 100 mL of distilled water. MNPs/ montmorillonite and zeolite were synthesized as follows: 5.50 gm of the synthetized magnetic iron merged with 20 grams of montmorillonite and zeolite in 250 ml of alcohol. Then, remove the precipitations and washed with distilled water several times and put in the oven to dry. Then, the dried product passed through a paper filter and the prepared nanoparticles were used for the experiments associated with the adsorption of the metallic ions under study. In general, the formation of magnetic iron nano-particles followed this reaction as shown in equation (1)

$$Fe^{2+} + 2Fe^{3+} + 8NH_3{\cdot}H_2O \longrightarrow Fe_3O_4\downarrow + 8NH_2 + 4H_2O \quad (1)$$

Noteworthy to mention that when ammonia is added to the $FeCl_2$ and $FeCl_3$ solutions, $Fe(OH)_2$ is initially formed (Eq. 1), which is then oxidized to Fe_3O_4 (Eq. 2). The formation mechanisms of Fe_3O_4 magnetic NPs can be summarized as follows:

$$Fe^{2+} + 2NH_3 + H_2O \rightarrow Fe(OH)_2 + 2NH_4^+, \quad (2)$$

$$3Fe(OH)_2 + 1/2O_2 \rightarrow Fe_3O_4 + 3H_2O \quad (3)$$

During the synthesis, magnetite in the dry state is oxidized to maghemite by air. It is known that ultrafine crystals of magnetite change over years from black to the brown of maghemite even at room temperature [33]. Also, the role of surfactants (also referred to here as ligands) such as oleic acid used in this case usually binds to the surface of the nanocrystals and give rise to a steric hindrance to aggregation. This method has widely been used because of the ease and reproducibility of the synthesis, as well as the uniformity, high crystallinity, and mono-dispersity of the product. Also, because of the dependence of photocatalytic and photo electrochemical properties on the nano particle size, significant efforts have been concentrated on the precise control of particle size distribution. Addition of purified montmorillonite and zeolite mixture (1:1) to Fe^{+2} and ferric ions solution with vigorous stirring at 150 ppm at temperature up to 40^0C for to get on homogenous solution. Then addition with addition of NH_4OH with drop wise of NaOH to get on precipitation of IMNPs on solution. The inorganic salt of ferric ion reacts with NH_4OH and forms FeOOH, which, upon heating, further produce into Fe^{2+} and OH^- ions, which consequently assists in the development of Fe_3O_4 ions according to the chemical reactions. The nanocomposite mixture has larger surface area than individual nanoparticles. These advantages increase the reduction percent of removal heavy metals and COD/BOD and other pollutants.

2.4. Wastewater pollutants Analysis

Total Kejeldahl Nitrogen (TKN), Ammonia (NH_3^+), Nitrite (NO_2^-) and Nitrate (NO_3^{-2})

Total Nitrogen (TN) =

R-N (Organic Nitrogen) + NH_3^+ + NO_2^- + NO_3^{-2}.

All components that comprise total nitrogen are biochemically interconvertible, are components of the nitrogen cycle, and can occur in both wastewater and natural waters (Standard Methods) [34].Transfer 50 mL of sample 50 mL into a 125 ml flask and add 1 m of 11 N sulfuric acid. Then, add 0.4 g ammonium persulfate, mix and boil for approximately 30-40 minutes. Then heat for 30 minutes in an autoclave at 121°C. Cool and dilute to 40 ml and filter. For each sample analyzed, including quality control samples, record the volume filtered and oven dry mass in the appropriate places. Calculate TSS using equation.

$$TSS\ (mg/L) = (A - B)/V$$

Where: A = mass of filter + dried residue (mg), B = mass of filter (tare weight) (mg), and V = volume of sample filtered (L) [35].

2.5. Characterization of modified nanocomposite (Sample Instrumentation)

The XRD pattern of nanocomposite Montmorillonite and Zeolite/IONPs was obtained using a X-ray diffractometer Schimadzu model: A PAN analytical

X-rays diffraction equipment model Expert PRO with secondary mono-chromator, Cu-radiation (λ=1.54A^0) at 50k.v.,40 M.A and scanning speed 0.02^o /sec. saturation magnetization of nanocomposite estimated by a vibrating-sample magnetometer (VSM, Homade 2tesla). A magnet (Φ 17.5×20 mm, 5500 O e) was utilized for the collection of magnetic particles. Coercivity, remanence and saturation of samples have been estimated. FT-IR spectroscopy were measured in a transmission mode on a spectrophotometer (PerkinElmer Spectrum Version 10.03.09) Spectrum Two Detector $LiTaO_3$ was used for separating the solid and liquid during the preparation samples. The samples were pressed pellets of a mixture of the powder with KBr. The micrographs of nanocomposite were obtained using SEM Model Quanta 250 FEG (Field Emission Gun). A plasma-atomic emission spectrometer (ICP-AMS, Optima 3000XL, Perkin Elmer) used for detecting the concentrations of trace metal ions. Chemical Oxygen Demand (COD) is a measure of the biologically available and inert organic matter that is susceptible to oxidation by a strong oxidizing agent. COD method is based on the well-established closed dichromate-reflux colorimetric method. The sample is added to the reagent vial, digested under closed reflux conditions, and allowed to cool before measurement is taken. COD is used to estimate pollutants of wastewater to measure the efficiency of the treatment processes. This professional, waterproof meter complies with IP67 standards and measures DO barometric pressure, BOD and temperature. The METTLER TOLEDO portable TOC analyzer ensures system compliance with fast and simple point of use monitoring.

2.6. Batch Adsorption optimization Experiments

The experiments of adsorption of different pollutants on nanocomposite montmorillonite and zeolite/IONPs were performed by batch techniques. The effect of pH (3-8), contact time (30-90 min) and adsorbent dose (2-10 g/l) was screened in detail. Samples filtered before each test (Whatman filter) to prevent of turbidity interference in experiment results. The methods of (4500-B), (Vanadate - molybdate), (5210-A) and (5210-B) for Standard Methods for the Examination of Water and Wastewater used to determine final amounts of different pollutants. [36]

Adsorption percentage was calculated using the following equation.

$$\% \text{ Removal} = (Ci - Cf)/Ci * 100 \quad (1)$$

In this equation Cf and Ci are the initial and final concentration of heavy metals in solution, respectively. Then the following equation was used to determine the adsorption capacity:

$$qe=(C_0-C_e)\ V/M \quad (2)$$

In this equation qe is adsorption capacity and C_0 and C_e are initial and balanced concentration of heavy metals in liquid phase (mg/l). V is volume of the solution (L) and M is the amount of used adsorption (g)

Table 1. The initial BOD, COD, TOC, TSS, TN and TP concentrations were determined in untreated wastewater

Parameter	Unit Concentration	Concentration
COD	mg/L	656.70
BOD	mg/L	587.09
TSS	mg/L	125.43
TOC	mg/L	490.32
TN	mg/L	76.40
TP	mg/L	16.74

2.7. Isotherm studies

In general, adsorption isotherm models are explained to detect the maximum uptake capacity of an adsorbent and to identify the adsorption mechanism. The experimental part of this study was performed by shaking, for 30 min at room temperature and in a thermostatic water bath shaker, 15.0 mg of the prepared magnetic nanocomposite with several 100 ml pollutant ions aliquots of different concentrations; ranged from 25 to 200 mg/L. The pH of all solutions was adjusted to 7.0. After shaking, magnetic nanocomposite was separated and the remaining concentration of carbonaceous compounds was determined by the aforementioned method. Langmuir and Freundlich isotherm were examined to analyze the collected data. Langmuir model assumes monolayer adsorption of the adsorbate at homogeneous binding sites on the adsorbent surface [37]. Freundlich model supposes multi-layer adsorption of the adsorbate on the heterogeneous surface of the adsorbent [38].

2.8. Kinetic studies

Kinetic models were examined to see which evaluate the current adsorption process. The experimental part of this study was performed as follows: at room temperature and in a thermostatic water bath shaker, 15.0 mg of magnetic nanocomposite was shaken, separately, with different concentration of carbonaceous compounds ions solution for different time intervals. The pH of all solutions was adjusted to 7.0. After shaking, magnetic nanocomposite was separated and the remaining concentration of carbonaceous compounds ions was determined by the aforementioned method [39].

2.9. Thermodynamic studies

The thermodynamic nature of an adsorption process is generally deduced from the numerical values of three thermodynamic parameters, Gibbs free energy (ΔG^o), standard entropy change (ΔS^o) and standard enthalpy change (ΔH^o). Mathematically, these parameters are calculated from equations listed in Table 13. Data required for the thermodynamic study were collected by shaking 15.0 mg of the adsorbent with 100 mL solution at different temperatures (from 303 to 323 K) for 30 min. The amount of carbonaceous compounds ions in the filtrate was detected by the aforementioned procedure [40].

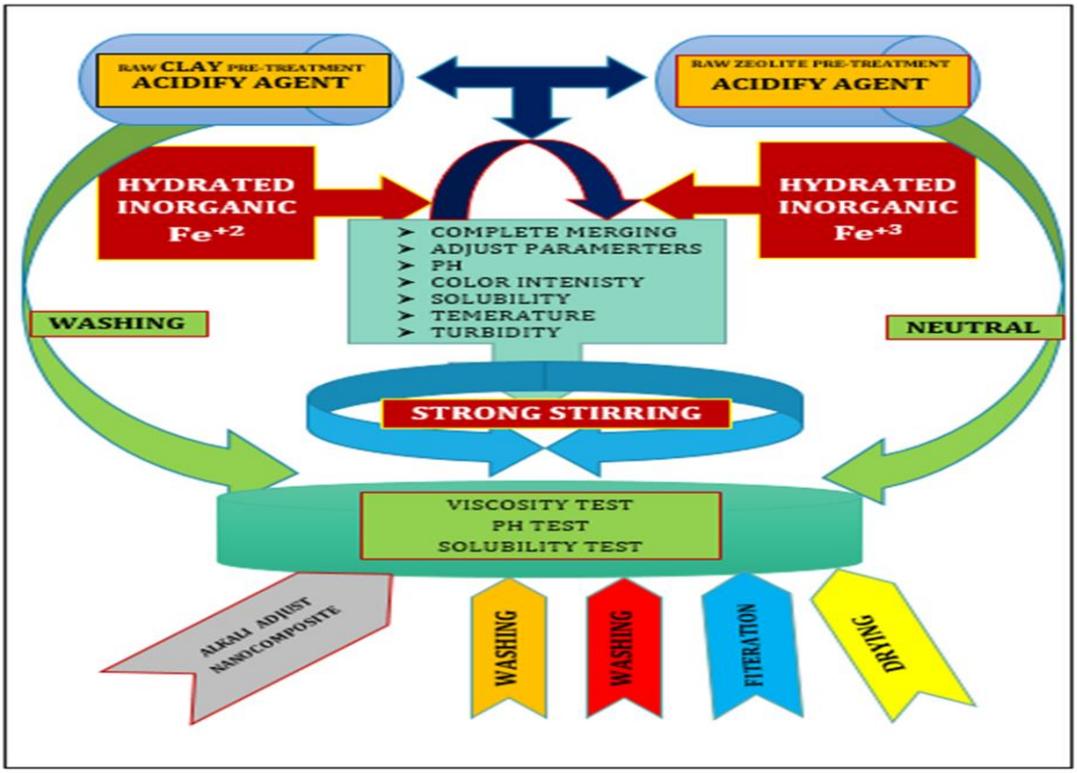

Fig. 1 Schematic illustration methodology of nanocomposite montmorillonite and zeolite/IONPs

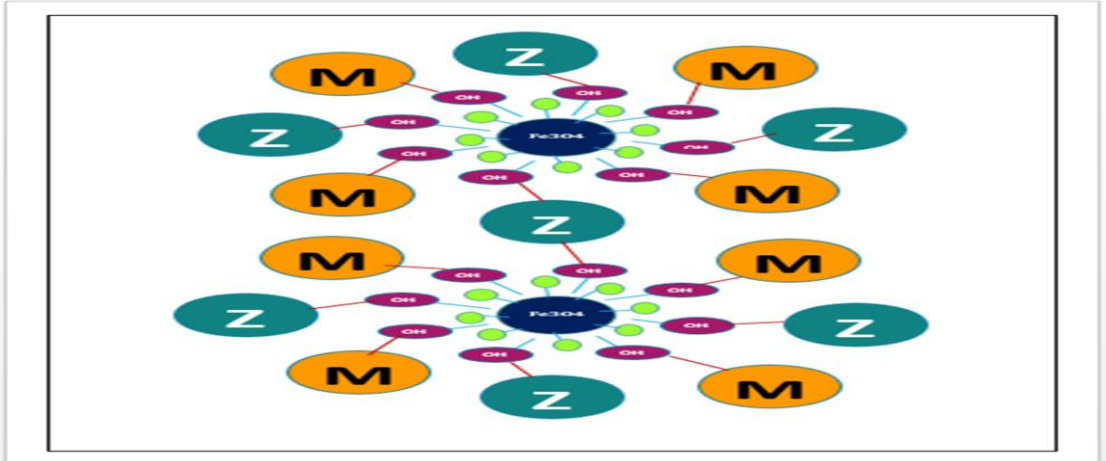

Fig. 2 Hypothetical Schematic structure of nanocomposite montmorillonite and zeolite/IONPs

3. RESULTS and DISCUSSION

3.1. Evaluation of acidification minerals before and after treatment by montmorillonite and zeolite /IONPs

Table 2. Showed the chemical composition of different oxide compounds which connected with each other's by tetragonal and octagonal structures as in Montmorillonite shape. The silicates as shown in (table 2) looks like as core element for different shapes so, it had a high percent and so on. The different crystallographic shapes of Montmorillonite and Zeolite Minerals participate in increasing the surface area, and also improvement the removal efficiency of varies pollutants. Acidification technique for mineral clay purification was the simplest and cheapest chemical method. It is revising mainly on different concentration of HCl to remove varies soluble chloride salts after treatment to get on purified phase of Montmorillonite and Zeolite Minerals.

Table.2 Chemical Constituents of Montmorillonite and Zeolite Minerals Before and After Acidified Purification by X-ray Fluorescence (XRF)

Chem. %	RMON. B.T.	RMON. A.T.	RZEO. B.T.	RZEO. A.T.
SiO_2	53.40	69.70	61.23	69.00
Al_2O_3	23.70	20.03	11.73	17.23
Fe_2O_3	5.30	3.25	1.88	0.33
CaO	1.50	0.83	2.34	1.38
Na_2O	1.92	0.71	1.55	0.60
MgO	0.27	0.10	1.21	0.14
K_2O	1.24	0.49	1.72	0.55
others	10.67	4.89	12.94	10.77

(A) Raw montmorillonite before treatment (RMON. B.T)(B) Raw montmorillonite after treatment (RMON. A.T) (C) Raw zeolite before treatment (RZEO. B.T) (D) Raw zeolite after treatment (RZEO. A.T)

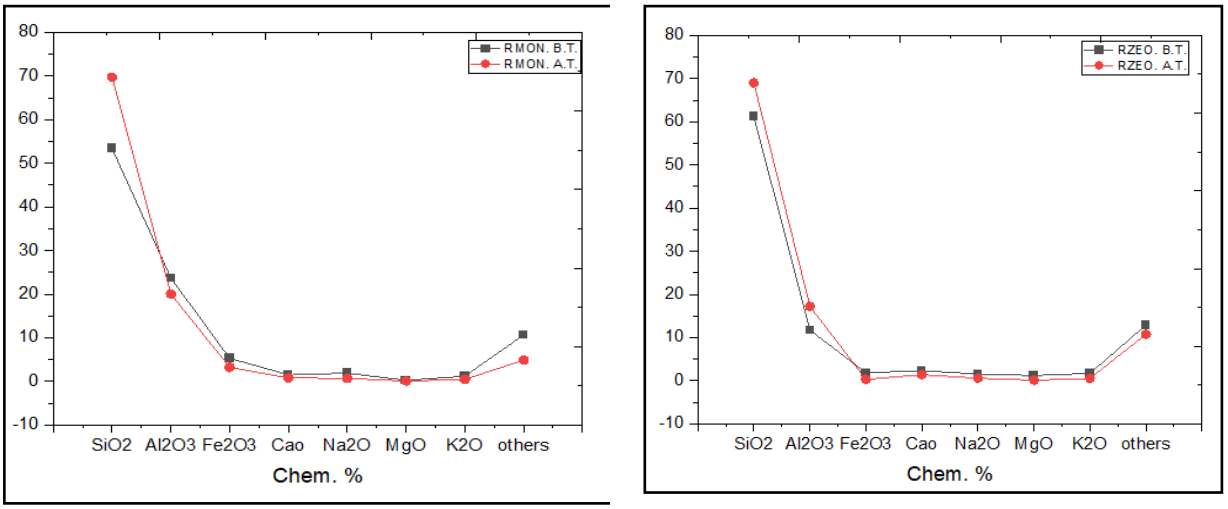

Fig. 3 Chemical Constituents of Montmorillonite and Zeolite Minerals Before and After Acidified Purification by X-ray Fluorescence (XRF)

3.2. Characterization of the montmorillonite and zeolite /IONPs

3.2.1. Assessment of x-ray diffraction analysis (XRD)

Figure 4. Showed the different sharp peaks intensity at varies 2 thetas at 15.50, 22.50, 30.10, 32.50, 41.20, 45.50, 53.50. The positions and relative intensities of the reflection peak of Fe_3O_4 and Fe_2O_3 MNPs agree with the XRD diffraction peaks of iron oxide nanoparticles. The peak of zeolite appears on 15.50 according to standard peak of zeolite. Broad peaks showed at 41.20, 45.50 related to new nanocomposite (Zeo-Mon-IONPs) formed. These peaks indicated to

success nanocomposite formed with high efficiency and new crystallographic shapes formed [41].

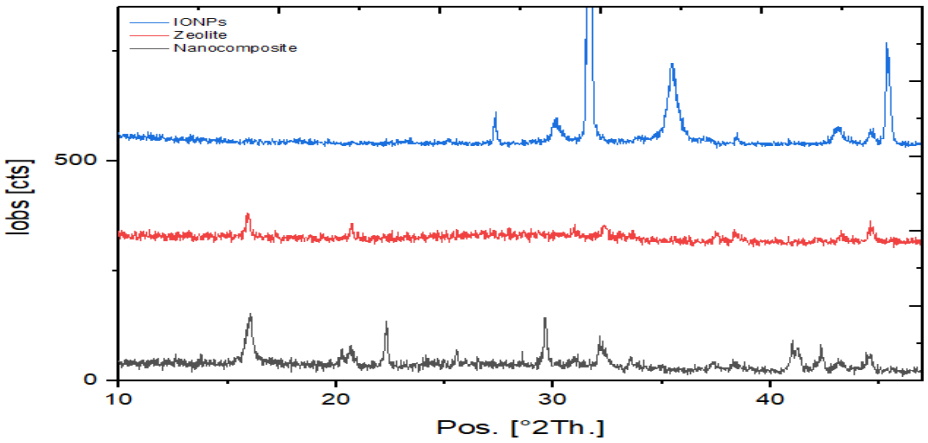

Fig. 4 XRD pattern of montmorillonite and zeolite /IONPs

3.2.2. Scanning electron microscope (SEM) of montmorillonite and zeolite/ IONPs

Fig. 5 showed that surface area of nanocomposite Montmorillonite and Zeolite/IONPs and, which confirms that the cubic and spherical shape of nanocomposite IONPs nanoparticles Montmorillonite and Zeolite merged in bending structure. The SEM photos showed the effect of iron salts to form nano-pellets with different shapes. By using mixing of inorganic salts gave rounded nanoparticles with larger surface area. Photo A and D show the big surface area of nanocomposite montmorillonite and zeolite/IONPs with holes that adsorption process occurred [42].

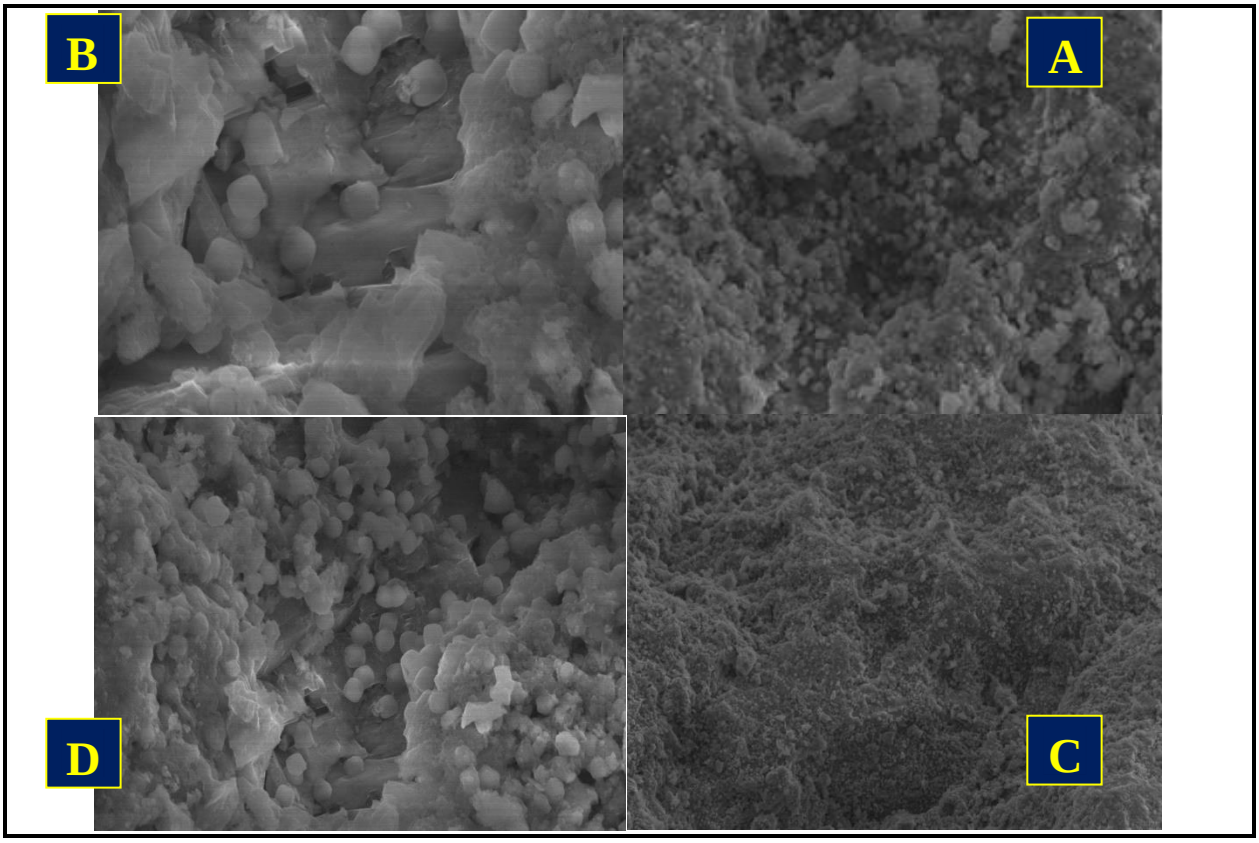

Fig. 5 Scanning Electron microscope photos of montmorillonite and zeolite /IONPs

3.2.3. IR spectroscopy of montmorillonite and zeolite /IONPs

As in Figure (6) Absorption peaks at 510 cm^{-1} and 540 cm^{-1} indicated to the Fe–O vibration related to the iron oxide in nano-sized and two absorption peaks at 2,924 and 2,854 cm^{-1} were attributed to the asymmetric CH_2 stretching and the symmetric CH_2 stretching, respectively. The bands due to C–O stretching mode were merged in the very broad envelope centered on 1250 cm^{-1} arising from C–O, C–O–C stretches and C–O–H bends vibrations of iron oxide nanoparticles. The aliphatic C–H stretching, in 1320 and 1390 cm^{-1} were due to C–H bending vibrations [43]. The sharp band at 530-660 cm^{-1} is likely due to the vibration of the Si–O bonds. The IR band at 3455 cm^{-1} can be assigned to the stretching modes of surface H_2O molecules or to an envelope of hydrogen-bonded surface OH groups. Specifically, two absorption bands located between 600 and 1000 cm^{-1} attributed to the bending of silica linkages and vibration of silica-alumina linkages, were detected; an absorption peak at a wavelength of 1250 cm^{-1} attributed to the stretching of silica can also be detected. The IR band at 3455 cm^{-1} was attributed to the molecules of hydrated water within the structure of silica-alumina. However, the intensities of the above mentioned peaks varied from one structure to another. A change in the intensity of a certain absorption band is an indication of the associated differences between the compared structures. The formation of iron oxide nanoparticles within the structure of silica-alumina was further confirmed by the bands observed at 1100, 1350, 2000, 3250, and 3500 cm^{-1}. These peaks are indicative of the tetrahedral silicate molecules. Similarly, the intensities of montmorillonite and zeolite/IONPs peaks, which are located at 1980, 2011, and 2093 cm^{-1}. Vibrations of the frameworks of zeolites give rise to typical bands in the mid and far infrared. A distinction is made between external and internal vibrations of the original assignments of the main IR bands were as follows: 1130 – 1035 cm^{-1} related to Si-O and asymmetrical stretch 1104 cm^{-1} showed to Al-O. Symmetrical stretch (503 - 525 cm^{-1}) bend to Si-O-Al. (450 - 401 cm^{-1}) double ring vibrations related to the interaction between (Si-O-Al). Sharp peak appears at 871 cm^{-1} indicate to new linkage asymmetrical stretching band of Si-O-Fe/Al-O-Fe. The concept of strictly separated external and internal tetrahedral vibrations must be modified in that zeolite framework vibrations appear to be strongly coupled. Hydroxyl groups attached to zeolite structures are most important for the chemistry of these materials [44]. They may be detected and characterized by IR spectroscopy as such due to their vibration modes. IR spectroscopy is extensively used to characterize minerals as adsorbate systems. Adsorption and desorption of water (hydration and dehydration) may be easily monitored by IR, since adsorbed H_2O gives rise to a typical deformation band around 1421 cm^{-1}.

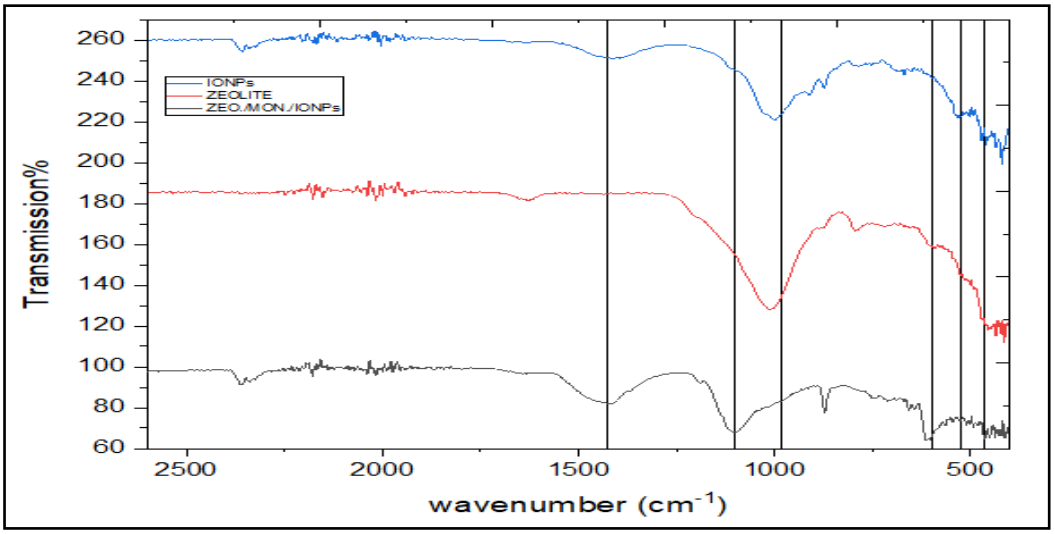

Fig. 6 IR-Spectroscopy of nanocomposite Montmorillonite and Zeolite/IONPs

3.2.4. Magnetic characterization of nanocomposite (VSM)

Vibrating sample magnetometer (VSM) will help to understand the magnetic properties of the prepared samples. The low hysteresis in the magnetization showed that produced nanoparticles had paramagnetic strength [45]. The saturation magnetization values of IONPs, Zeo. /IONPs, Mon. /IONPs and nanocomposite Montmorillonite and Zeolite/IONPs were 32.395 emu/g, 0.85358 emu/g, 3.38509 emu/g and 0.64710 emu/g respectively. Figure. 7 indicated that IONPs had high MS values than others. This was due to the complex crystallographic shapes of clay and zeolite which reduce the MS values massively [46].

Table. 3 VSM measurements values for nanocomposite montmorillonite and zeolite/IONPs

parameters	IONPs	Zeo./ IONPs	Mon./IONPs	Zeo./ Mon./IONPs
Coercivity (Hci)	250.41 G	569.21 G	623.80 G	625.56 G
Magnetization (Ms)	32.395 emu/g	0.85358 emu/g	3.38509 emu/g	0.64710 emu/g
Retentivity (Mr)	6.124 emu/g	0.18880 emu/g	0.18535 emu/g	0.12324 emu/g

IONPs: Iron oxide nanoparticles; Zeo. / IONPs: zeolite/IONPs; Mon./IONPs: Montmorillonite/IONPs

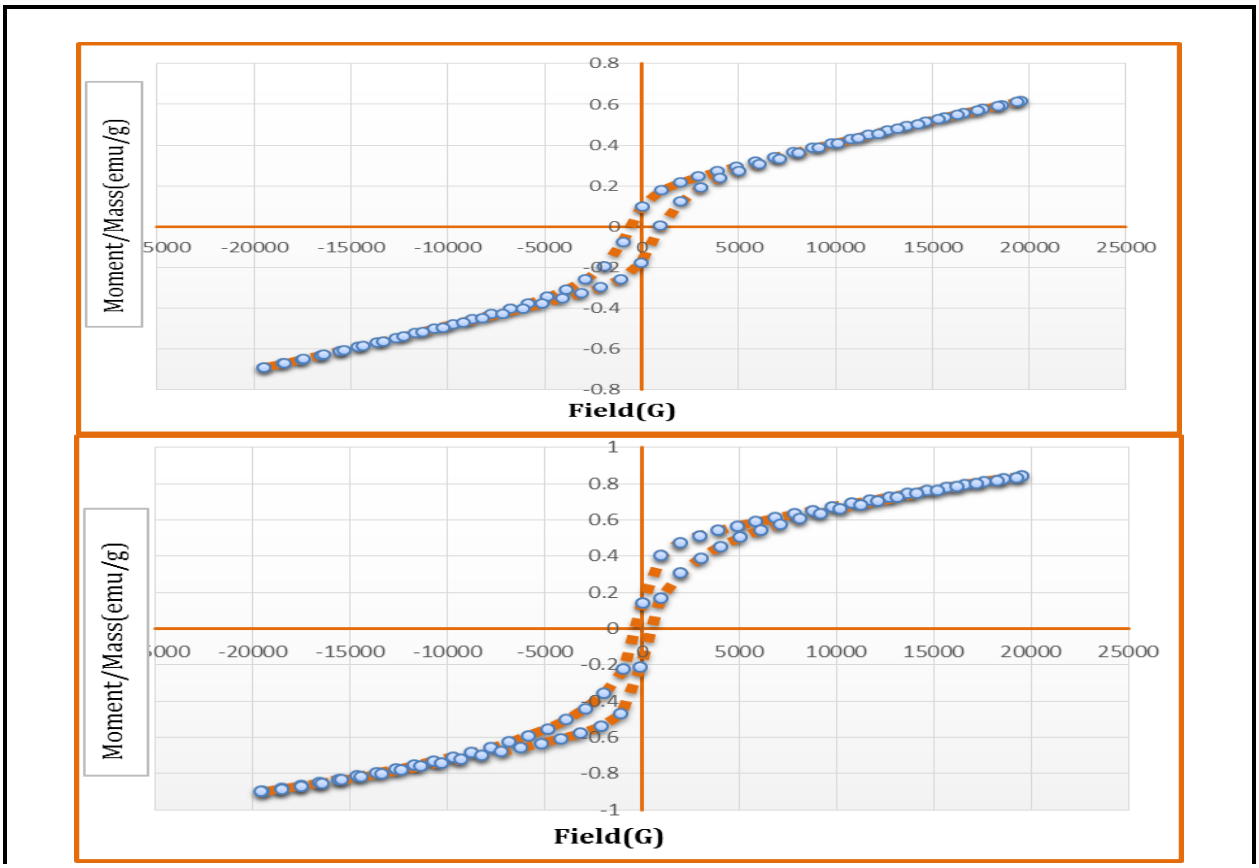

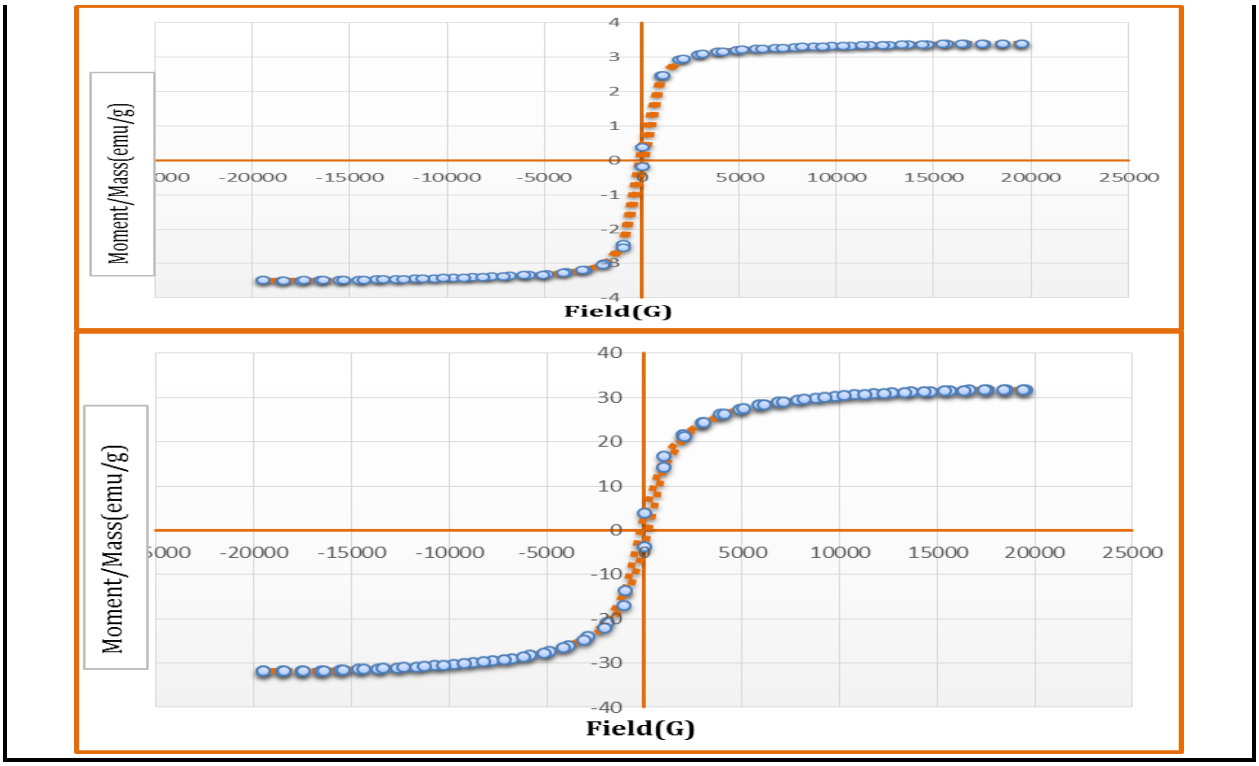

Fig. 7 A). (Ms) nanocomposite montmorillonite and zeolite/IONPs. B). (Ms) nanocomposite montmorillonite/IONPs. C). (Ms) Zeolite/IONPs. D). (Ms) IONPs.

3.2.5. Particle size analysis of nanocomposite montmorillonite and zeolite/IONPs)

Fig.5.shoed that the mean particle size and morphology of montmorillonite and zeolite/IONPs showed that the nanocomposite is nearly spherical and crystalline in shape. The nanoparticles intensity weighting was 62.40 nm, volume weighting was 22.90 nm and number weighting was 10.50 nm. The mean diameter of nanocomposite material ranges around 31.90 nm. This reading means that the obtained results of reduction percent of prepared Montmorillonite and Zeolite/IONPs depends mainly on the size and shape with availability of dispersion percent in solution. The particle size distribution test depends mainly on the increase of surface area and thus, increasing of removal efficiency.

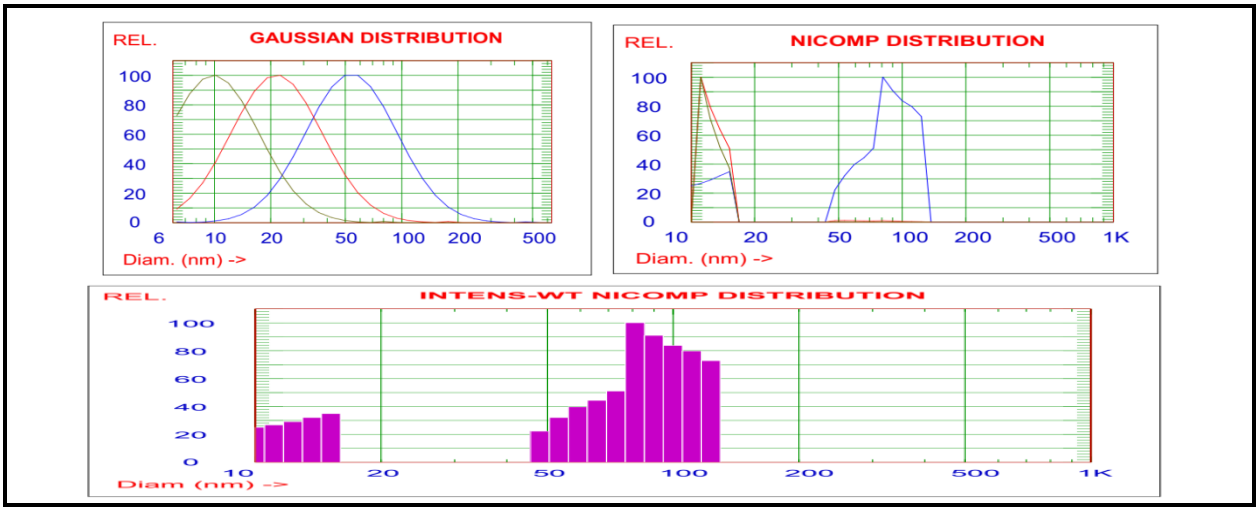

Fig. 8 Particle size distribution (Nano-sized) of nanocomposite montmorillonite and zeolite/IONPs

3.3 Adsorption Study of COD, BOD, TOC, TN, TSS and TP adsorption on nanocomposite montmorillonite and zeolite/IONPs

3.3.1. Effect of Initial pH

The pH plays an effective role in the removal of pollutants from wastewater. The pH was adjusted to the desired pH using the best value of nanocomposite Montmorillonite and Zeolite/IONPs dosage was 5 g/l.

Table. 4 Relation between pH and reduction% of different pollutants

pH	Reduction %					
	COD	BOD	TOC	TSS	TN	TP
3	55	60	52	52	45	40
4	62	73	60	61	60	55
5	83	90	79	82	76	70
6	80	85	82	73	81	76
7	75	82	71	61	70	73
8	73	80	70	54	68	64

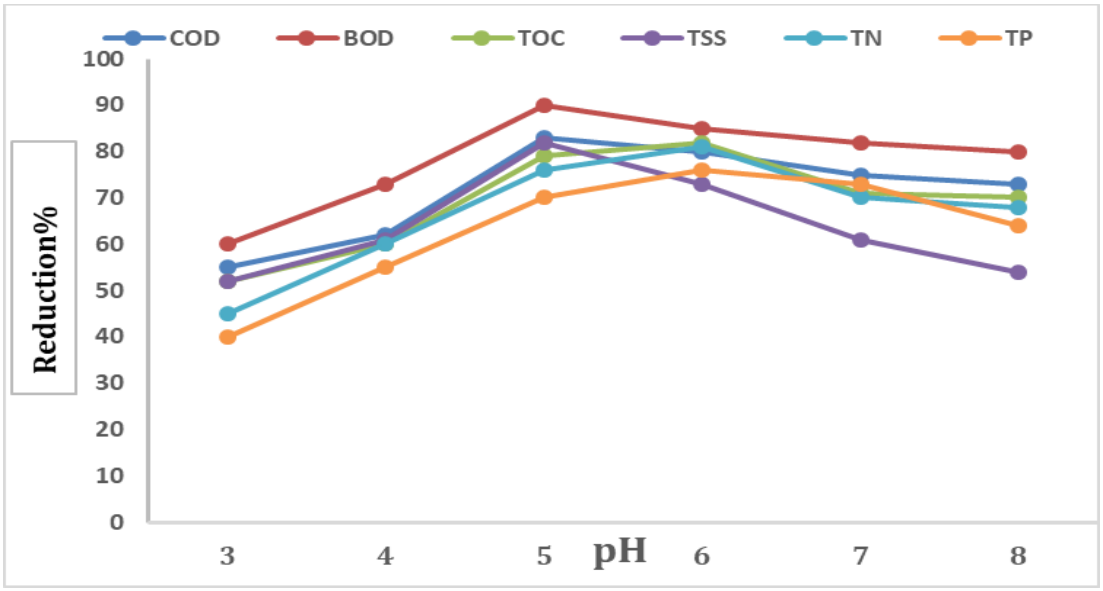

Fig. 9 Influence of pH on the removal of COD, BOD, TOC, TSS, TN and TP from Montmorillonite and Zeolite/IONPs nanocomposite. Doses 5 g/L, contact time 60 min.; Temp. 60 ^{0}C.

3.3.2. Effect of Montmorillonite and Zeolite/IONPs nanocomposite doses

The removal of COD, BOD, TOC, TSS, TN and TP with Montmorillonite and Zeolite/IONPs nanocomposite doses was determined, by using different concentration of nanocomposite from 2 to 10 g/L as illustrated in figure 10. It was observed that the Montmorillonite and Zeolite/IONPs nanocomposite efficiency increased with increasing doses up to (5 g/L), after that the Montmorillonite and Zeolite/IONPs nanocomposite efficiency declined with increasing doses. At the optimal Montmorillonite and Zeolite/IONPs nanocomposite doses (5 g/L), the removal of COD, BOD, TOC, TSS, TN and TP were 81%, 92%, 86%, 80%, 73% and 75% respectively. The increase of the nanocomposite efficiency with increasing nanocomposite doses was obtained probably due to the increase of positive charged metal ions concentrations to neutralize negative charge organic particles. A head of the optimal nanocomposite doses, the reversal charge took place on the surface of the nanocomposite particles with the excess amount nanocomposite doses, and hence the decline of the increase of nanocomposite efficiency.

Table. 5 Relation between nanocomposite Doses and reduction % of different pollutants

Doses. g/L	Reduction %					
	COD	BOD	TOC	TSS	TN	TP
2	42	51	55	45	40	42
3	65	68	67	59	50	53
4	73	83	71	70	60	66
5	81	92	86	80	73	75
8	80	91	84	78	71	74
10	79	90	82	77	70	73

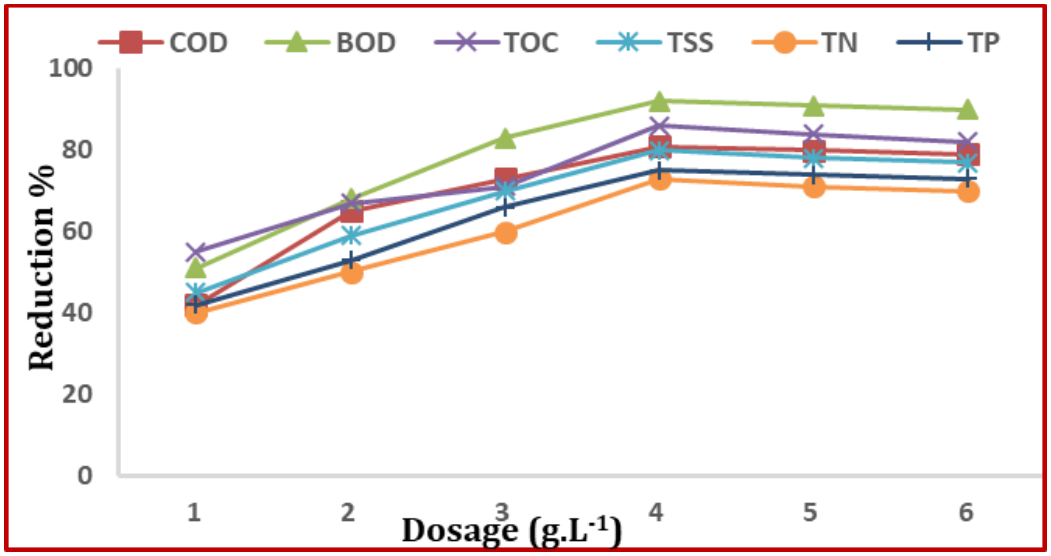

Fig. 10 Influence of nanocomposite dosage on the removal of COD, BOD, TOC, TSS, TN and TP from Montmorillonite and Zeolite/IONPs; pH 5; contact time 60 min.; Temp. 60 ^{0}C.

3.3.3. Effect of Contact Time on Montmorillonite and Zeolite/IONPs nanocomposite with different pollutants

The contact time plays an important role on the removal of organic pollutants from wastewater. The influence of the nanocomposite efficiency on the removal of COD, BOD, TOC, TSS, TN and TP were determined, as presented in figure 3. The removal of COD, BOD, TOC, TSS, TN and TP increased with time, up to 60 min. The removal efficiency increased for COD, BOD, TOC, TSS, TN and TP were 82%, 88%, 81%, 83%, 81%, and 84% respectively at the 60 min treatment time.

Table. 6 Relation between contact time and reduction % of different pollutants

Contact time	Reduction %					
	COD	BOD	TOC	TSS	TN	TP
5	40	38	36	29	46	43
15	54	61	49	45	59	61
30	65	74	66	67	67	72
45	70	83	76	74	76	76
60	82	88	81	83	81	84
75	80	85	80	81	79	82
90	79	84	79	77	78	80

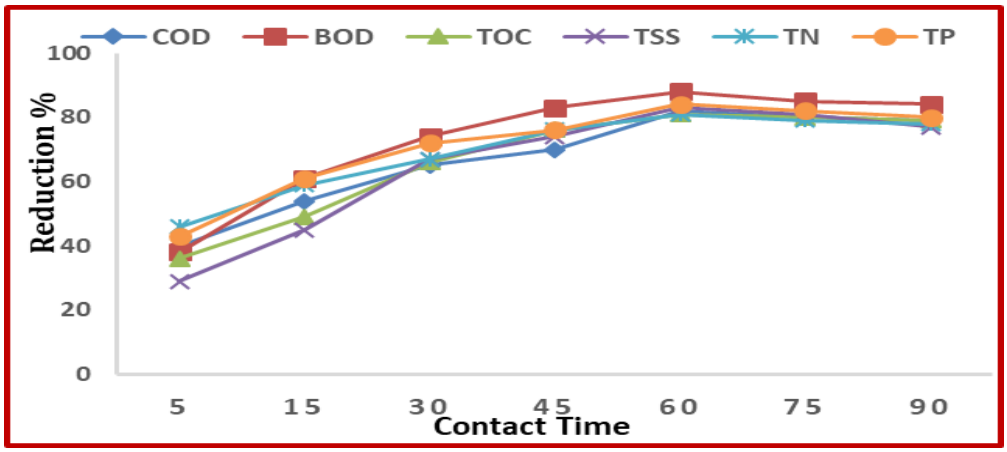

Fig. 11 Influence of contact time on the removal of COD, BOD, TOC, TSS, TN and TP from Montmorillonite and Zeolite/IONPs. Doses 5 g/L, pH 5; Temp. 60 ^{0}C.

3.3.4. Effect of Contact Time on Montmorillonite and Zeolite/IONPs nanocomposite with different pollutants

The removal of COD, BOD, TOC, TSS, TN and TP using nanocomposite was determined with different temperatures (40 ± 1 ◦C) to 80 ◦C, as presented in figure 5. The removal of COD, BOD, TOC, TSS, TN and TP rapidly increased with increasing temperature and reached maximum at 60 ◦C, however, the removal efficiency was decreased with a further increase of temperature above 60^{o}C. The maximum removal of COD, BOD, TOC, TSS, TN and TP were obtained at 70^{o}C. The increased nanocomposite efficiency with increasing temperature which was observed could be due to the decrease of viscosity with dispersion rate of the organic compounds in pollutants.

Table. 7 Relation between Temp. ^{0}C and reduction % of different pollutants

Temp. ^{0}C	Reduction %					
	COD	BOD	TOC	TSS	TN	TP
40	79	85	76	81	77	80
50	85	91	82	86	80	86
60	94	93	89	91	89	89
70	90	92	87	89	87	82
80	89	88	85	85	82	80

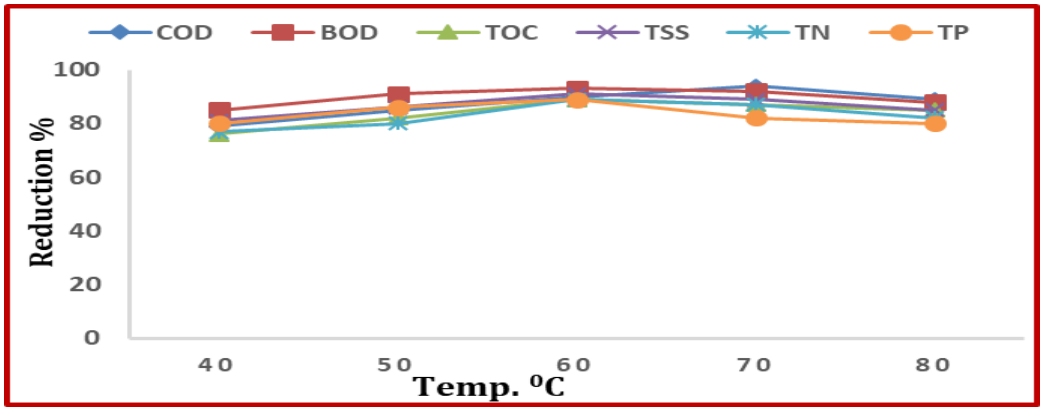

Fig. 12 Influence of temperature on the removal of COD, BOD, TOC, TSS, TN and TP from Montmorillonite and Zeolite/IONPs. Doses 5 g/L, pH 5; contact time 60 min.

3.4. Chemical treatment of wastewater pollutants by nanocomposite montmorillonite and zeolite/IONPs

Table (8) showed that the total nitrogen values in wastewater samples before treatment was 76.40 ppm and 20.06 ppm after treatment. On the other hand. This may be due to the real that the larger ammonium ions content had a difficult purpose because only a certain quantity of negative loads exists and was available of oxygen atom in the zeolite structure. And also, certain quantities of pores exist in the mineral, which it has possible to join with a smaller percentage of molecules that contains a higher ammonium concentration. The total phosphorous value of a sample before treatment was 16.74 ppm and the value reduced to 4.92 ppm after treatment. This may be due to the fact that nanocomposite Montmorillonite and Zeolite/IONPs possesses a specific capacity of pores for the adsorption of substances, and when a greater amount of phosphorus is present, not all the phosphorus can be adsorbed in a similar way as previously outlined for ammonium. In phosphorus removal, besides the dependence shown with its own concentration in the medium, a slight dependence with the ammonium concentration was also observed when this concentration was increased in the medium. This may be due to the fact that, because of the attraction of loads that exists among these positive ions, ammonium enters the pores of the mineral before the other molecules to the sectors where negative loads generated by oxygen atoms are present [47].

Table. 8 Chemical analysis of polluted wastewater before & after treatment of nanocomposite montmorillonite and zeolite/IONPs

Parameters	TN / ppm	TP /ppm
Before treatment	76.40	16.74
After treatment	20.06	4.92
Reduction %	73.74	70.60

3.5. Chemical treatment of polluted (TSS, COD, BOD and TOC) of wastewater sample by nanocomposite montmorillonite and zeolite/IONPs

COD values are almost always higher than BOD values for the same sample. As a result, the multiplication factor will usually be less than one. Once established, the correlation will only apply to the sample used to create it (one couldn't use the correlation with samples taken from other water sources). The amount of oxygen required (COD or BOD) may change while the carbon concentration (reflected by the TOC value) does not. Industrial influent wastewater it could vary from 1.67 and 6.65 and influent sewage it could be in range of 2 to 3. Treated effluent COD: TOC ratio might be same or change based on type of treatment. These ratios vary based on type of wastewater and need to be standardize for particular type of wastewater stream. Table (9) showed that the raising of TSS (total suspension solids) in collected wastewater sample. The TSS value before treatment by nanocomposite Montmorillonite and Zeolite/IONPs was 125.43 ppm and this value was high. After treatment the reading value was 26.07 ppm and reduction % value was 79.21%. COD (Chemical Oxygen Demand) was the most popular alternative test to BOD for establishing the concentration of organic matter in wastewater samples. COD value before treatment was 656.70 ppm and after treatment by nanocomposite Montmorillonite and Zeolite/IONPs was 110.78 ppm and reduction % value was 83.13%. BOD (Biochemical Oxygen Demand) is the traditional, most widely used test to establish concentration of organic matter in wastewater samples (i.e., relative strength). BOD value before treatment was 587.09 ppm and after treatment by nanocomposite Montmorillonite and Zeolite/IONPs was 68.01 ppm and reduction % value was 86.12 % [48].

Table. 9 Chemical Analysis of polluted wastewater before & after treatment of nanocomposite montmorillonite and zeolite/IONPs

Parameters	TSS	COD	BOD_5	TOC
	ppm			
Before Treatment	125.43	656.70	587.09	490.32
After Treatment	26.07	110.78	70.02	68.01
Reduction %	79.21	83.13	88.07	86.12

3.6. Study the relations ratios between COD/BOD and TOC

Extensive observation of the COD and BOD levels on the same wastewater has shown that the COD to BOD ratio of a particular wastewater will remain constant over time. The mean average range of COD/BOD ratio was 1.25. COD/BOD ratios can be highly variable. The more variable the ratio values, as in, the higher the COD/BOD ratio, the greater the percentage of slowly biodegradable and non-biodegradable material in the sample and that means the BOD_5 test will give a lower value than is truly representative of the oxygen demand in the sample. The ratio value of COD/TOC was 1.34 before and 1.63 after treatment respectively. This means that presence of some undesirable materials complex carbonous materials in wastewater sample. The ratio value of TOC/BOD_5 was 0.84 before treatment and 0.97 after treatment. The same concept in table 5 that after treatment by nanocomposite montmorillonite and zeolite/IONPs showed increase in ratio value. The COD/BOD_5 ratio of the effluent prepared semi synthetically wastewater treatment plant was 1.12. However, after treatment with nanocomposite montmorillonite and zeolite/IONPs. The effluent or floating liquid of this process increased the value to 1.34. This result can be attributed to a higher removal of COD than of BOD_5 probably due to the fact that before the application of nanocomposite montmorillonite and zeolite/IONPs removal, certain compounds may have hindered the process of biological degradation developed during the BOD^5 test but that were adsorbed by the nanocomposite montmorillonite and zeolite/IONPs.

Table. 10 Relation between pollutants ratios before and after treatment by nanocomposite montmorillonite and zeolite/IONPs

Parameters	COD/BOD_5 ratio	COD/TOC ratio	TOC/BOD_5 ratio
Before Treatment	1.12	1.34	0.84
After Treatment	1.58	1.63	0.97

3.7. Recovery and reusability of adsorbents

Reusability of nanocomposite adsorbents can reduce the cost of technical operation of removing several pollutants. In wastewater treatment technologies, is to get on materials that have a high adsorption capability without deterioration that may be easily removed from the polluted media. Regeneration of the nanocomposite is the big important operation to check availability of nanocomposite sorption. The economic feasibility is out target, it is estimated that such ingredients could be used for several cycles without dropping their adsorption capacity, or at least with slight loss. In this paper, ten successive adsorption–desorption series operated. Reusability of pollutants adsorbed on Zeo. / Mon. /IONPs was carried out using 0.1 M HCl with continuous shaking at 180 rpm for 1 h at 25 C. The values achieved using Zeo. / Mon. /IONPs after ten adsorption–desorption series are shown in Fig. 13. The regeneration stability was edited on applying the adsorption and desorption procedures numerous times. The experiment displays that a significant decrease in the sorption capacity after 8 repeating cycles. The sorption removal capacity of TN decreases from 73.74% to 72.54%, 70.40%, 68.12%, 66.11%, 64.03%, 63.65%, 62.69%, and 60.45% and also, for the sorption removal capacity of TP decreases from 70.60% to 68%, 66%, 65%, 63%, 61%, 60%, 60% and 55%. The sorption removal capacity of COD decreases from 83.13% to 82%, 80%, 78%, 77%, 76%, 75%, 74%, and 73% respectively. The sorption removal capacity of BOD from 88.07% to 87%, 86%, 85%, 84%, 83%, 81%, 81% and 80% respectively. The sorption removal capacity of TOC from 86.12% to 85%, 84%, 83%, 82%, 81%, 80%, 78% and 77% respectively. The result showed that the synthesized Zeo. / Mon. /IONPs could be successfully used for treating wastewater pollutants at least for eight times.

Table. 11 The relation between reusability cycles and different pollutants of nanocomposite Zeo. / Mon. /IONPs

Pollutants	Reusability cycles/Removal efficiency (%)							
	1	2	3	4	5	6	7	8
TN	72	70	68	66	64	63	62	60
TP	68	66	65	63	61	60	60	55
COD	82	80	78	77	76	75	74	73
BOD	87	86	85	84	83	81	81	80
TOC	85	84	83	82	81	80	78	77

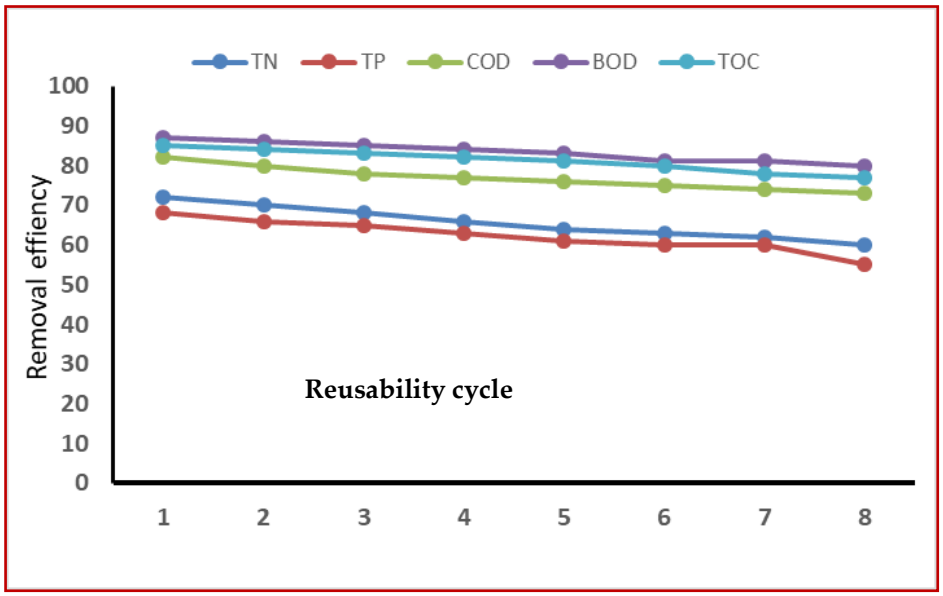

Fig. 13 Effect of reusability on the efficiency of Zeo. / Mon. /IONPs towards removal pollutants at optimal conditions.

3.8. Study the Adsorption isotherm and Equilibrium Studies

The adsorption equilibrium studies reflect the dependence of the amount of adsorbate particle on the surface of synthetized nanocomposite. Longmuir, Freundlich, and BET models are the mathematical model equations that are used to determine the quantity of adsorbate particles and the nature of adsorption. An adsorption study was conducted to model the experimental data obtained from the effect of the process variables for the removal of COD, BOD, TOC, TSS, TN and TP. The specific surface area of a powder is determined by physical adsorption of a gas on the surface of the solid and by calculating the amount of adsorbate gas corresponding to a monomolecular layer on the surface. Physical adsorption results from relatively weak forces (van der Waals forces) between the adsorbate gas molecules and the adsorbent surface area of the test powder. The determination is usually carried out at the temperature of liquid nitrogen. The amount of gas adsorbed can be measured by a volumetric or continuous flow procedure. [49, 50].

Table. 12 Parameters derived from both Langmuir and Freundlich fitting models for adsorption

	Langmuir Isotherm				Freundlich Isotherm			BET Model		
	q_m (mg/g)	K_L	R_L	R^2	1/n	K_f	R^2	R^2	A	$X_{m(mg/g)}$
COD	0.295	-0.897	-43.89	-0.897	0.295	0.701	0.866	0.996	34.58	0.23
BOD	0.493	6.689	335.47	6.689	0.493	1.070	0.969	0.995	60.24	0.75
TOC	0.595	7.345	368.26	7.345	0.595	1.179	0.916	0.992	38.31	0.56
TSS	0.571	9.528	477.41	9.528	0.571	0.851	0.947	0.983	36.10	0.48
TN	0.560	12.730	637.98	12.730	0.562	0.691	0.910	0.980	50.47	0.68
TP	0.562	11.280	565.30	11.280	0.566	0.701	0.960	0.990	42.70	0.59

qe (mg g^{-1}) is the adsorbed quantity of carbonaceous compounds ions at equilibrium per unit mass of magnetic nanocomposite, Ce (mg L^{-1}) is equilibrium concentration, q_m (mg.g^{-1}) is the theoretical adsorption capacity, K_L is Langmuir constant, K_F and n are Freundlich constants, $X_{m\ (mg/g)}$ (amount of adsorbate adsorbed by the coagulant to form a monolayer), *A* (interaction energy between adsorbate and coagulant surface), correlation coefficients (R^2).

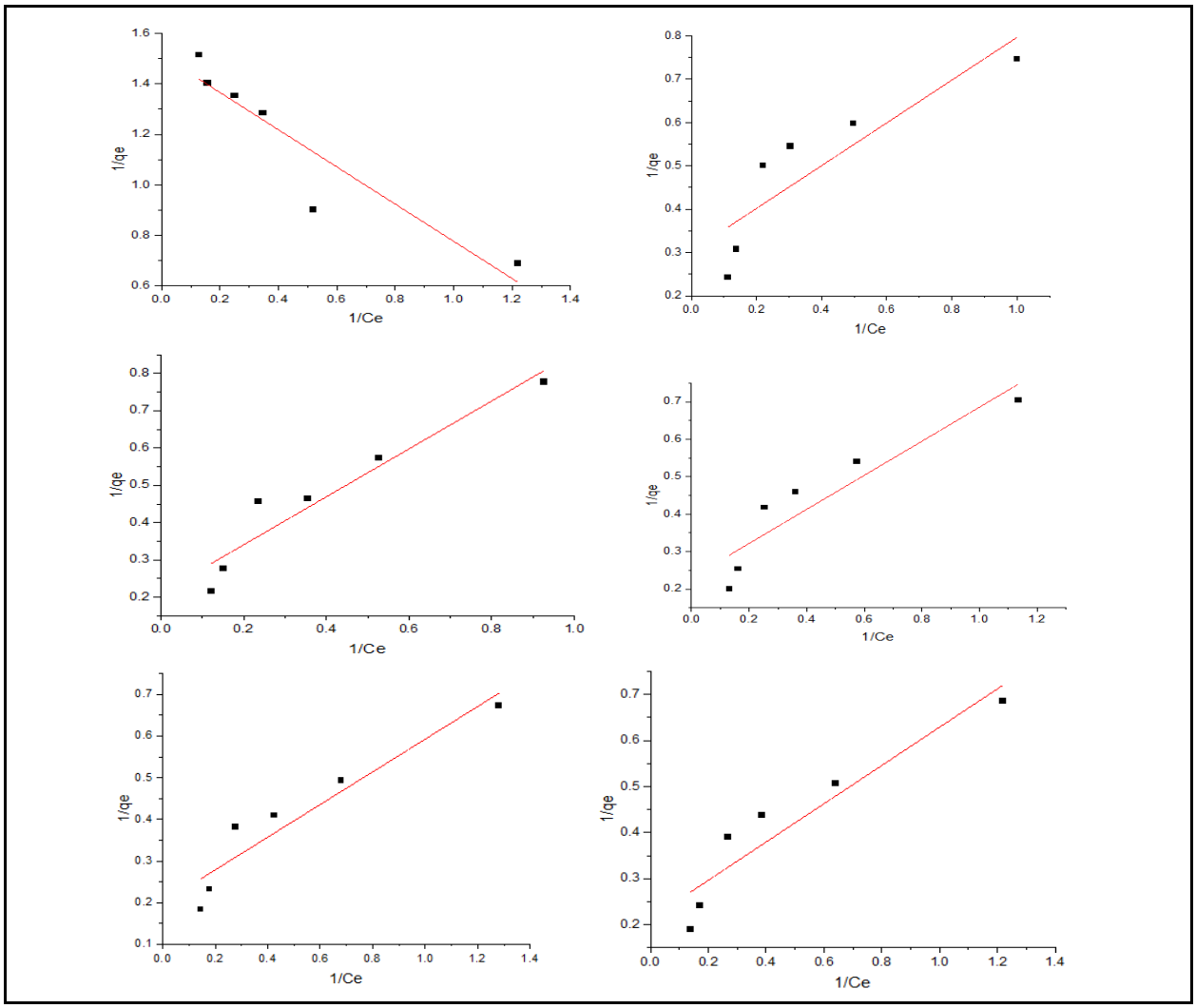

Fig. 14 Langmuir adsorption isotherm modeling for the removal of (a) COD; (b) BOD; (c) TOC; (d) TSS; (e) TN and (f)TP by Zeo./ Mon./IONPs

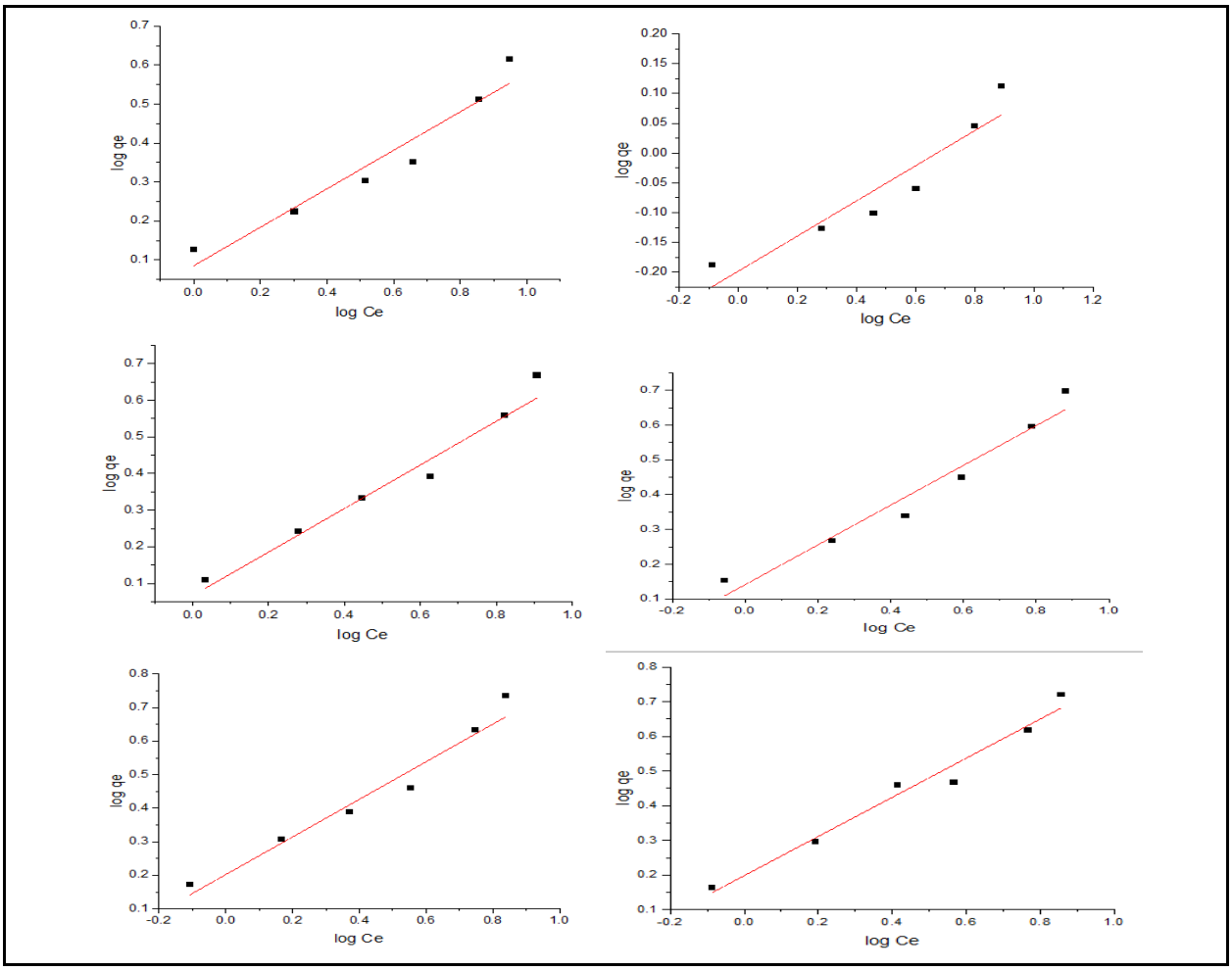

Fig. 15 Fendlish adsorption isotherm modeling for the removal of (a) COD; (b) BOD; (c) TOC; (d) TSS; (e) TN and (f)TP by Zeo./ Mon./IONPs

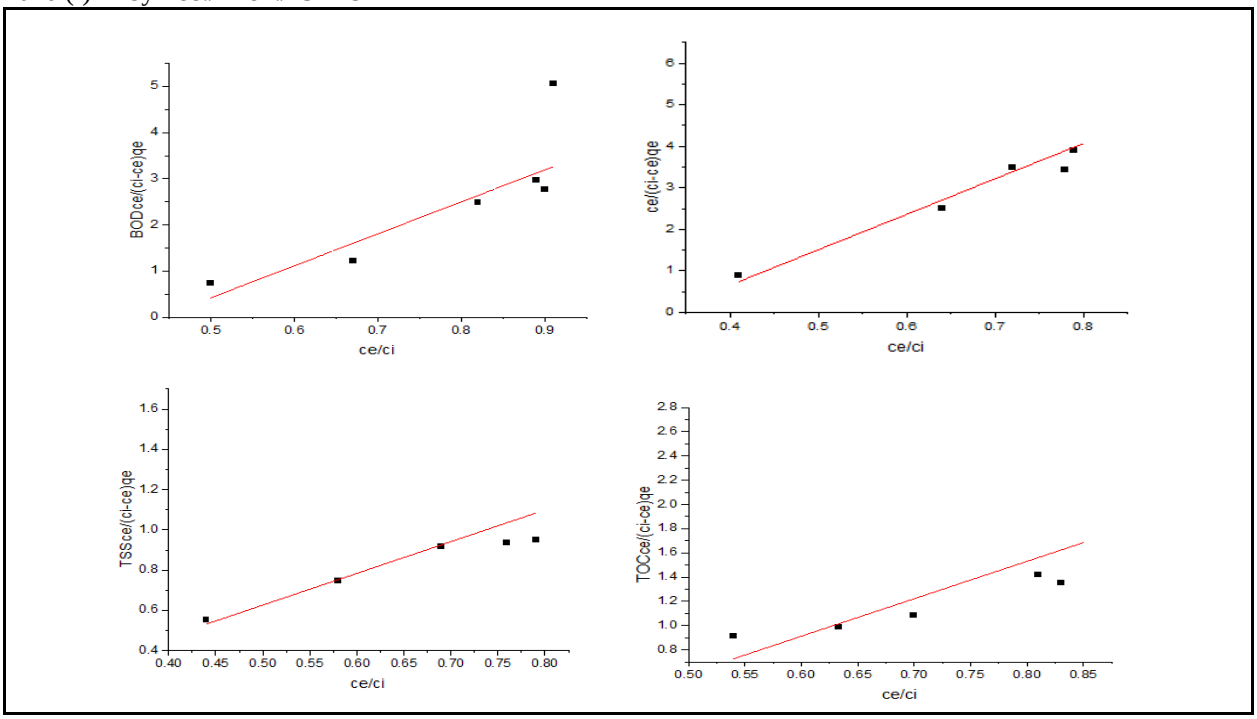

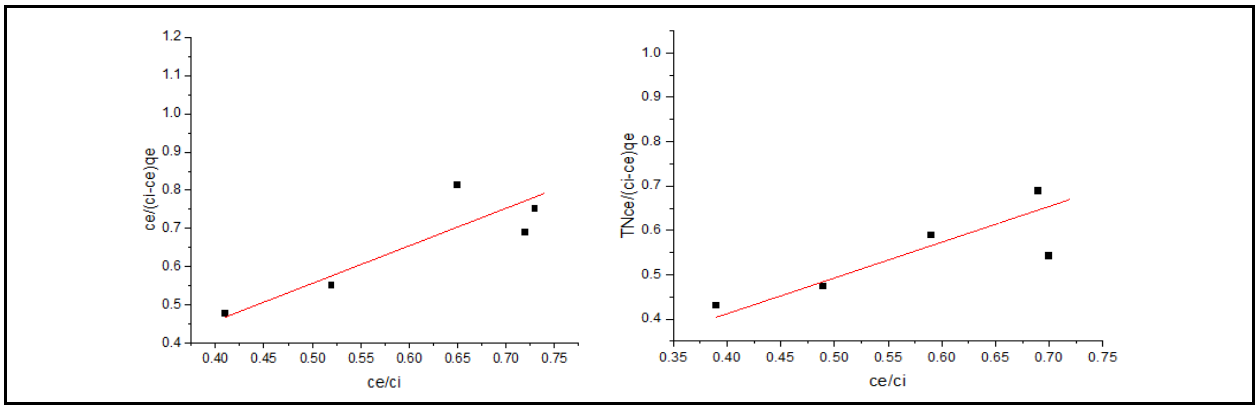

Fig. 16 BET adsorption isotherm modeling for the removal of (a) COD; (b) BOD; (c) TOC; (d) TSS; (e) TN and (f) TP by Zeo. / Mon. /IONPs

3.9. Effect of temperature and adsorption isotherm thermodynamics and kinetics

Reaction temperature is known to affect adsorption efficiency [51]. In this research, adsorption experiments were performed at different temperatures and optimal condition of nanocomposite dosage at certain pH. The temperature dependences of C_e and q_e are shown in fig.14**.** As the temperature increased from 30 to 80^0C, the pollutant removal rate slightly increased. This indicated that the adsorption of pollutant on nanocomposite was favored at high temperature, which suggested that the adsorption process was endothermic. Moreover, thermodynamic analysis revealed the occurrence of chemisorption, the extent of which is known to increase with increasing temperature because of the concomitant facilitation of diffusion [52]. In contrast, the reaction temperature had little effect on the adsorption efficiency, which agreed with previously obtained results. The effect of temperature on pollutants adsorption was further studied by thermodynamic analysis using Eqn. (12) – (15) to determine changes in the Gibbs free energy (ΔG), enthalpy (ΔH), and entropy (ΔS): [53, 54]

$$K_L = qe / Ce \quad (1)$$

$$\text{Ln } K_L = \Delta S/ R - \Delta H/ RT \quad (2)$$

$$\Delta G = \Delta H - T\Delta S \quad (3)$$

$$\Delta G = - RT \ln K_L \quad (4)$$

Where K_L is the adsorption distribution constant (L.g-1). ΔH and ΔS were obtained from the plot of ln K_L vs. 1/T (Fig.14) which allows for the determination of ΔG. Table 11 lists the obtained thermodynamic parameters and the calculated correlation coefficients, and shows that the adsorption ΔH was positive. This indicated that the adsorption of pollutants on nanocomposite was endothermic and chemical in nature. The positive value of ΔS suggested that adsorption increased randomness at the solid–liquid interface. The ΔG values were negative and decreased with increasing temperature, which indicated that adsorption was spontaneous in nature. Furthermore, the increase in ΔG with increasing temperature suggested that the adsorption of pollutants on nanocomposite was more favorable at higher temperatures. Negative value of Gibb's free energy shows the thermodynamic feasibility and spontaneity of the sorption process. The positive value of ΔH^o confirmed the endothermic nature of iron sorption. Positive value of enthalpy indicated that the increased randomness at the solid solution interface during the fixation of adsorbates on the active sites of the adsorbent. The influence of the nanocomposite particle size on the iron and manganese adsorption capacity revealed that the adsorption capacity for ions increased with the decrease of the nanocomposite particle size. These results were attributed to the increase of the nanocomposite surface area with the decrease of the particle size. Our findings regarding the correlation between the particle size, surface area and arsenic removal efficiency proved to agree with other reported studies. More than that, in agreement with other related studies the higher adsorption capacity for carbonaceous compounds ions obtained for nanocomposite was attributed to the high specific surface area of these nanoparticles [55].

Table. 13 Thermodynamic parameters for different pollutants sorption on the adsorbent

	Pollutants	Temp. (K)	K_L	ΔG^0 (KJ.mole^{-1})	ΔH^0 (KJ.mole^{-1})	ΔS^0 (KJ.mole^{-1})	R^2
Adsorbent	COD	313	0.949756	0.13414	38.9828	-127.162	0.8428
		323	0.37125	2.66092			
		333	0.256667	3.76518			
		343	0.165	5.13822			
		353	0.175443	5.10791			
	BOD	313	1.34	-0.76160	26.1826	-82.2456	0.8786
		323	0.832537	0.49217			
		333	0.559512	1.60767			
		343	0.438901	2.34832			
		353	0.451111	2.33625			
	TOC	313	1.191852	-456.722	19.7697	-61.8709	0.9076
		323	0.918947	226.989			
		333	0.768571	728.745			
		343	0.516471	1884.224			
		353	0.544819	1782.332			
	TSS	313	1.612727	-1.2437	22.4419	-68.5893	0.8782
		323	1.064138	-0.1669			
		333	0.789275	0.6551			
		343	0.605823	1.4291			
		353	0.638701	1.3157			
	TN	313	1.904103	-1.6758	22.7063	-67.6095	0.9129
		323	1.380816	-0.8665			
		333	1.034915	-0.0950			
		343	0.728889	0.9018			
		353	0.768571	0.7725			
	TP	313	1.779024	-1.4990	22.6340	-68.1459	0.8996
		323	1.263077	-0.6271			
		333	0.878462	0.3587			
		343	0.691351	1.0525			
		353	0.709863	1.0057			

where K_L is the distribution coefficient, q_e (mg.g^{-1}) is the uptake capacity at equilibrium and C_e (mg.L^{-1}) is the equilibrium concentration of the adsorbate and ΔG^o (kJ mol^{-1}) is the change in Gibb's free energy, ΔS^o (J/mol K^{-1}) is the change in standard entropy, ΔH^o (KJ/mol) is the change in standard enthalpy, T (K^0) is the kelvin temperature and R (8.314 J mol^{-1} K^{-1}) is the general gas constant.

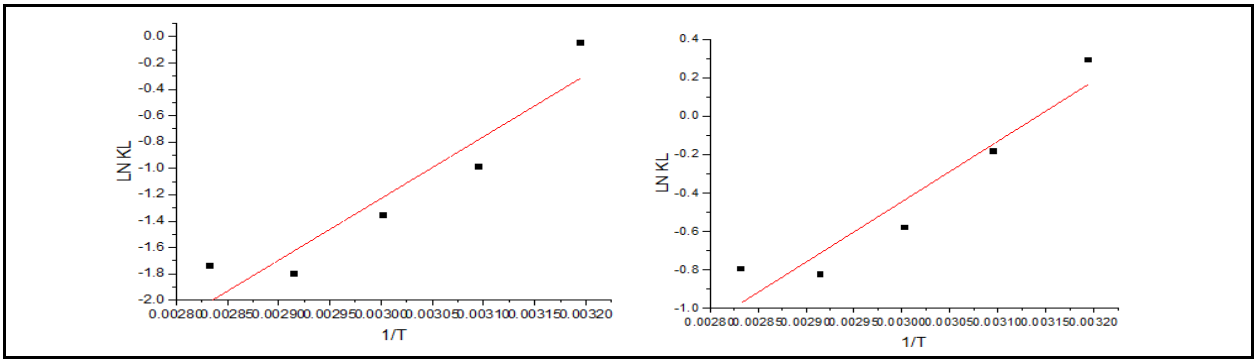

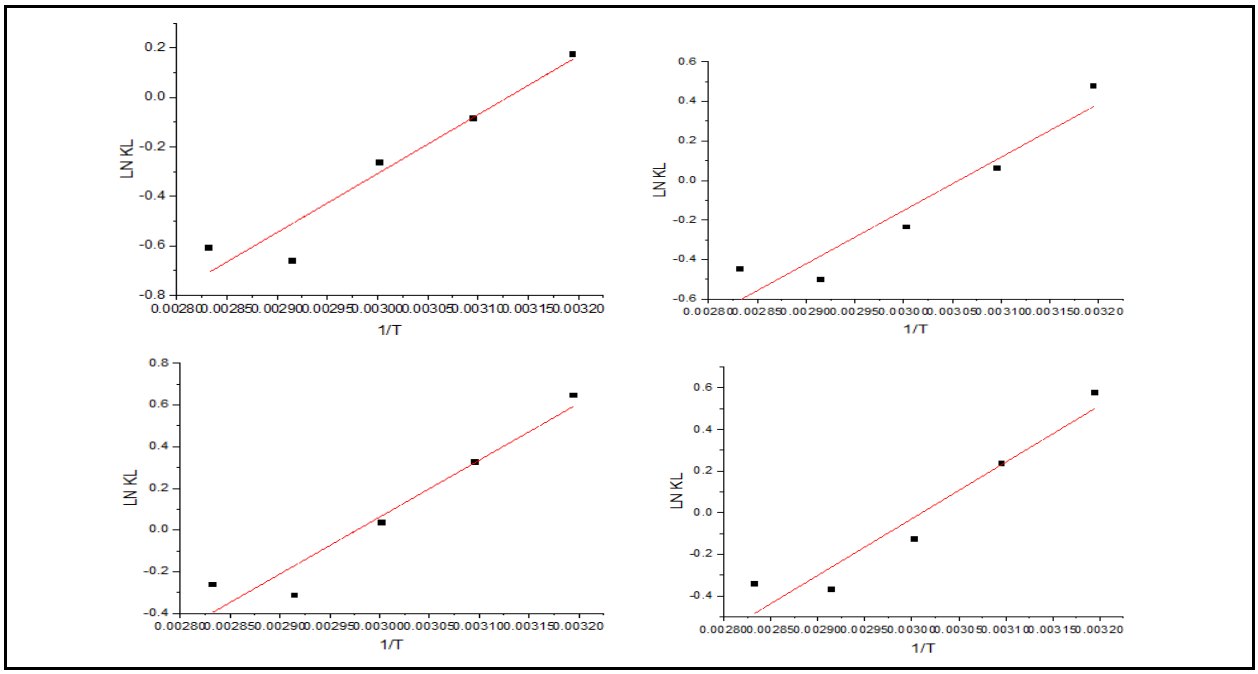

Fig. 17 Thermodynamic plots for different pollutants sorption onto nanocomposite adsorbent (plot of ln K_L versus 1/T)

4. Conclusions

In summary, the novality of this paper was in how to overcome the treatment of raw organo-philic clay and raw zeolite. The crystallographic shaped of montmorillonite and zeolite had different structure in tetragonal and octagonal shapes. The X-ray fluorescence (XRF) analysis showed SiO_2 and Al_2O_3 as main components of natural zeolite and local montmorillonite. These shapes depend mainly on Si-O and Al-O bonds, these bonds gave more of active sites on oxygen atoms and hydroxyl groups. The co-precipitation method for synthesis of iron oxide in nanoscale was occurred under adsorption process. We obtained on new nanocomposite which contained on supported treated minerals (montmorillonite and zeolite) coated by several millions of negative oxygenated attached to magnetite and hematite as core. The mean average of nanocomposite formed by SEM images showed that the magnetite particles were successfully intercalated into the interior of between (montmorillonite and zeolite) and average dimeter of nanoparticles size was (12-62 nm) that contribute to get on high removal efficiency of different pollutants such as organic and inorganic matters as shown in this paper and polluted heavy metals. Optimal conditions of nanocomposite dosage were 5 g/l at contact time 30 min with temperature at 50 ^oC and PH solution 6.0. At lower pH, montmorillonite and zeolite/IONPs adsorbent represented as an excellent adsorbent. But, at higher pH than 7. It gave low adsorption values. The adsorption process involved electrostatic interaction between the protonated groups of montmorillonites and zeolite/IONPs surface and negative groups of organic matter, total nitrogen and total phosphates. This study focused on removal of COD/BOD and TOC and also total nitrogen & phosphates by adsorption and desorption processes. The results showed that the maximum percentage removal of COD, BOD, TOC and total suspended solids (TSS) by using nanocomposite montmorillonite and zeolite/IONPs was obtained was 83.13 % & 88.07 % and 86.12 respectively and for TN, TP and TSS was 73.74 % &70.60 % and 79.21 %. The ratio values between COD/BOD_5 & COD/TOC and TOC/BOD_5 were 1.58 &1.63 and 0.97. Adsorption data were successfully reproduced by the Langmuir isotherm, and also, carbonaceous compounds adsorption saturation capacity was determined as 72.04 and 206.611 $mg.g^{-1}$ respectively. The average adsorption free energy change calculated by adsorption isotherm model was 2.880 kJ mol^{-1}, which indicated the occurrence of ionic exchange. Overall, the thermodynamic parameters implied that

carbonaceous compounds adsorption was endothermic and spontaneous. Data derived from kinetics models meant that the adsorption process takes place via strong physical interactions, such as electrostatic attraction, hydrogen bonding and Vander Waal forces, between carbonaceous compounds ions and the adsorbent surface.

Reference:

[1]-Kostjukovs, J., Actiņš, A., Sarceviča, I., Karasa, J. Method for obtaining smectites from clay having low levels of smectites, EU patent No. EP2465820 B1, (2016).

[2]-Sarcevica, I., Kostjukovs, J., Actiņš, A. Enrichment and activation of smectite poor clay, *IOP Conf. Series. Materials Science and Engineering*, 23 (01236), (2011).
http://dx.doi.org/10.1088/1757-899X/23/1/012036

[3]-Bergaya, F., Lagaly, G. Surface modification of clay minerals, *Appl. Clay. Sci*., vol. 19, pp. 1–3, 2001. Doi.org/10.1016/S0169-1317 (01)00063-1(2016).

[4]-Sivakumar Durairaj. Experimental and analytical model studies on leachate volume computation from solid waste, *Int. J. Environ. Sci. Tech.*, 10, 903–916 (2013c).

[5]-Sivakumar, D. A study on contaminant migration of sugarcane effluent through porous soil medium, *Int. J. Environ. Sci. Tech.*, 8,593–604 (2011).

[6]-Kurniawan, A., Chan, G.Y.S., Lo, W.H, and Babel, S. Physico-chemical treatment techniques for wastewater laded with heavy metals, *Chemical Engineering Journal*, 118, , 83-98 (2006).

[7]-Hoda roushdy guendy. Treatment and reuse of wastewater in the textile industry by means of coagulation and adsorption techniques, *Journal of App. Sci. Res*., 6(8), 964-972 (2010).

[8]-Sivakumar, D., Kandaswamy, A.N., Gomathi, V., Rajeshwaran, R and Murugan, N. Bioremediation studies on reduction of heavy metals toxicity, *Pollution Research*, 33, 553–558 (2014e).

[9]-Shankar, D., Sivakumar, D., Thiruvengadam, M., Manojkumar, M., Cooler removal in a textile industry wastewater using coconut coir pith, *Pollution Research*, 33, 490–503 (2014a).

[10]-Sivakumar, Durairaj, Shankar, Durairaj. Colour removal from textile industry wastewater using low cost adsorbents, *International Journal of Chemical, Environmental and Pharmaceutical Research*, 3, 52–57 (2012).

[11]-Sivakumar, D., Shankar, D., Gomathi, V and Nandakumaar, A. Application of electro-dialysis on removal of heavy metals, *Pollution Research*, 33, 2014i, 627–637.

[12]-Sivakumar, D., Shankar, D., Vijaya Prathima, A.J.R., Valarmathi M. Constructed wetlands treatment of textile industry wastewater using aquatic macrophytes, International. *Journal of Environmental Science*, 3,1223–1232(2013a)

[13]-Sivakumar, D., Shankar, D., Kandaswamy, A.N and Ammaiappan, M. Role of electro-dialysis and electro-dialysis cum adsorption for chromium (VI) reduction, *Pollution Research*, 33, 547–552 (2014j)

[14]-Sivakumar, D., Shankar, D., Nithya S, Rajaganapathy J. Reduction of contaminants from leachate using *moringa oleifera*– A kinetic study, *Pollution Research*, 33, 529-529 (2014k).

[15]-Hansen, H.K., Nunez, P., Raboy, D., Schippacase, I., and Grandon, R. Electrocoagulation in wastewater containing arsenic: Comparing different process designs**.** *Electrochemical Acta*, 52, 3464-3470 (2007).

[16]-Tchamango, S., Nanseu-Njiki, C.P., Ngameni, E., Hadjiev, D., and Darchen, A. Treatment of dairy effluents by electro coagulation using aluminium electrodes, *Science of the Total Environment*, 408, 947-952 (2010).

[17]-Vasudevan, S, Lakshmi, J, and Sozhan, G. Studies on the removal of iron from drinking water by electrocoagulation – *A clean process, Clean: Soil, Air, Water,* 37, 45-51 (2009).

[18]-van Lier, J. B., Tilche, A, Ahring, B. H, Macarie, H, Moletta, R, Dohanyos, M. New perspectives in anaerobic digestion et al. *Water Sci. Technol*. 43,1–18 (2001).

[19]-Abudi, Z. N., Hu, Z., Sun N, Xiao, B., Rajaa, N., Liu, C. Batch anaerobic co-digestion of OFMSW (organic fraction of municipal solid waste), TWAS (thickened waste activated sludge) and RS (rice straw): influence of TWAS and RS pretreatment and mixing ratio. *Energy* 107, 131–140.
Doi: 10.1016/j.energy.2016.03.141 (2016).

[20]-Castillo, M. E. F., Cristancho, D. E., and Arellano, A. V. (2006). Study of the operational conditions for anaerobic digestion of urban solid wastes.*Waste Manage*. 26, 546–556.
Doi:10.1016/j.wasman (2005).

[21]-Carrere, H., Dumas, C., Battimelli, A., Batstone, D. J., delgenes, J. P., Steyer, J.P. et al. Pretreatment methods to improve sludge anaerobic digestion

degradability: a review. *J. Hazard Mater*. 183, 1–15 (2010).

[22]-Li, H., Li, C., Liu, W., and Zou, S. Optimized alkaline pretreatment of sludge before anaerobic digestion. *Bioresour. Technol*. 123, 189–194. Doi: 10.1016/j.biortech.2012.08.017 (2012).

[23]-Carlsson, M., Lagerkvist, A., and Morgan-Sagastume, F. The effects of substrate pretreatment on anaerobic digestion: a review. *Waste Manage*. 32, 1634–1650. Doi: 10.1016/j.wasman.2012.04.016 (2012).

[24]-López, Torres, M. and Espinosa Lloréns, Mdel, C. Effect of alkaline pretreatment on anaerobic digestion of solid wastes. *Waste Manage*. 28, 2229–2234. Doi: 10.1016/j.wasman.2007.10.006 (2008).

[25]-Modenbach, A. A., and Nokes, S. E. The use of high-solids loading in biomass pretreatment – a review. *Biotechnol. Bioeng*. 109, 1430–1442. Doi: 10.1002/bit.24464 (2012).

[26]-Neves, L., Ribeiro, R., Oliveira, R., and Alves, M. M. Enhancement of methane production from barley waste. *Biomass Bioenergy* 30, 599–603. Doi: 10.1016/j.biombioe.2005.12.003 (2006).

[27]-Ward, A. J., Hobbs, P. J., Holliman, P. J., and Jones, D. L. Optimization of the anaerobic digestion of agricultural resources. *Bioresour. Technol*. 99, 7928–7940. Doi: 10.1016/j.biortech.2008. 02.044 (2008).

[28]-Abdel-Raouf, N.; Al-Homaidan, A.A.; Ibraheem I.B.M. Microalgae and wastewater treatment. Saudi Journal of Biological Sciences, 19, 257- 275(2012).

[29]-El-Shatoury, E.H.; El-Liethy, M.A.; Abou-Zeid, M.A.; El-Taweel, G.E.; El-Senousy, W.M. Antibiotic susceptibility of Shiga Toxin Producing E. coli O157:H7 isolated from different water sources. The Open Conference Proceedings Journal. 6: 30-34(2015).

[30]-Hanan, A. Fouad., Rehab, M. Hefny., Al-moaataz Bellah M. M. Kamel. Mohamed Azab El-Liethy2 , Bahaa A. Hemdan2*. Assessment of Biological Augmentation Technology of Hazardous Pollutants Existing in Drainage Water in Bahr El-Baqar Drain, Egypt. Egypt. J. Chem. Vol. 63, No.7, pp. 2551 - 2563 (2020).

[31]-Kamalaldin, N.A.,Yahya, B.H., Nurazreena, A. Cell evaluation on alginate/hydroxyapatite block for biomedical application. *Procedia. Chem.* 19 297–303 (2016).

[32]-Magdy H. El-Sayed and Yasser A.M. Abdulhady. Heavy metals removal by using magnetic iron oxide/TiO_2 nanocomposite for wastewater treatment in 10th of Ramadan city, Egypt. *Egyptian J. Desert Res*., **65**, No. 1, 81-99 (2015).

[33]-Standard Methods for the Examination of Water and Wastewater, 20th Edition, 4500-N Nitrogen. 4-99-110 and 4-124-127.

[34]- Standard Methods for the Examination of Water and Wastewater. Method 2540 D, APHA, 21st Edition, (2005).

[35]-Cornell, R.M. and Schwertmann, U. Iron oxides. 2nd Edn, Wiley-VCH Verlagsgesellschaft Weinheim (2003).

[36]-Mahdavi, M, Namvar, F, Ahmad, M.B. and Mohamad, R. Green biosynthesis and characterization of magnetic iron oxide (Fe_3O_4) nanoparticles using seaweed (*Sargassum muticum*) aqueous extract. *Moecules*, 18: 5954–596 (2007).

[37]-Ahmadreza, Yazdanbakhsh., Akbar, Eslami., Mostafa, Gharloghi., Ehsan, Aghayani., Mohammad, Mehralian., Bahador, Amraei. The efficiency of iron oxide nanoparticles (Fe_3O_4 MNPs) loaded on zeolite as adsorbent for advanced treatment of secondary effluent: An insight of adsorption isotherm and kinetic. *International Journal of Pharmacy & Technology*. ISSN: 0975-766X CODEN: IJPTFI 290451484 (2015).

[38]-Nasser, H. Shalaby., Radwa, A., Elsalamony, Ahmed, M.A. El Naggar. Mesoporous Waste Extracted SiO_2-Al2O_3 Supported Ni and Ni-H3PW12O40 nano-Catalysts for Photo-degradation of Methyl Orange Dye under UV irradiation. April. *New Journal of Chemistry* 42(1)
DOI: 10.1039/C8NJ01479E (2018).

[39]- Choe, S., Chang, Y-Y., Hwang, K-Y., and Khim, J. Kinetics of reductive denitrification by nanoscale zero-valent iron. *Chemosphere.* 41(8):1307-11 (2000).

[40]-Huang, YH., Zhang, TC. Kinetics of nitrate reduction by iron at near neutral pH. *Journal of environmental engineering.* 128(7):604-11 (2002).

[41]- Suzuki M. Adsorption Engineering, 4th Edn, Kodansha, Tokyo. (1990).

[42]-Elı'as, Oliva., MarcosI, Vaschetto., Eliana Urreta, G., Silvia, E., Silvia, P. *Journal of Magnetism and Magnetic Materials* 322, 3438–3442 (2010).

[43]-Tamas Szab ´ o´, Aristides Bakandritsos, Vassilios Tzitzios, Szilvia Papp, Laszl ´ o K ´ or ″ osi , Gabor Galb ´ acs ´ , Kuanyshbek Musabekov, Didara Bolatova, Dimitris Petridis and Imre Dek ´

any ´. *Nanotechnology*. 18 285602 (9pp). DOI: 10.1088/0957 4484/18/28/285602 (2007).
[44]-Danková Zuzana1, Fedorová Erika1, Bekényiová, Alexandra1, Dankanova, Z. et al: Bentonite/iron. *Archives for Technical Sciences* 16(1), 65-75. DOI: 10.7251/afts.2017.0916.065D COBISS.RS-ID 6440472 (2017).
[45]-Habib, NR., Taddesse, AM., Temesgen, A. Synthesis, characterization and photocatalytic activity of $Mn_2O_3/Al_2O_3/Fe_2O_3$ nanocomposite for degradation of malachite green., *Bulletin of the Chemical Society of Ethiopia* 32 (1), 101-109 (2018).
[46]-Indira, T.K., Lakshmi, P.K. Magnetic nanoparticles - A review, *Int. J. Pharm. Sci. Nano-technol*., 3: 1035-1042 (2010).
[47]-World Health Organization, Manganese and its Compounds: Environmental Aspects: Concise International Chemical Assessment Document, World Health Organization, Geneva, Switzerland, (2004).
[48]-Wu, X.L, Guan, Y.T, Zhang, X, Huang, X, and Qian, Y. *Environ. Technol.* 23, 677–684 (2002).
[49]-Sivakumar, D., Rajaganapathy, J., Anand, R., Mariavensa, S., Preethi, S. *Journal of Chemical and Pharmaceutical Sciences*. ISSN: 0974/296124718 (2015).
[50]-Mehdinia, A., Shegefti, S., Shemirani, F. Removal of Lead (II), Copper (II) and Zinc (II) Ions from Aqueous Solutions Using Magnetic Amine-Functionalized Mesoporous Silica Nanocomposites. *J. Braz. Chem. Soc*. 26, 2249-2257 (2015).
[51]-Singh, S., Barick, K.C., Bahadur, D. Surface engineered magnetic nanoparticles for removal of toxic metal ions and bacterial pathogens. J. *Hazard. Mater*. 192, 1539– 1547 (2011).
[52]-Daou, O. Zegaoui and Amachrouq A. *Water Sci. Technol*. 75, 1098–1117. 42 K. K (2017).
[53]- Anoop and Anirudhan T. S. *J. Hazard. Mater*. 92, 161–183. 43 S. M. Awadh and F. H. Abdulla, Environ. *Earth Sci*. 76, 386. 44 H (2002).
[54]-Chen, Q. S., Huang, B., Wang, S. W. and Wang, L. Y. *J. Radioanal. Nucl. Chem.* 316, 71–80. 45 H (2018).
[55]-Moussout, A H., Aazza, M., Zegaoui, O., and A. C. El. *Water Sci. Technol.*73, 2199–2210 (2016).